



Review

# Recent Advances in Magnetite Nanoparticle Functionalization for Nanomedicine

Roxana Cristina Popescu<sup>1,2</sup>, Ecaterina Andronescu<sup>1</sup> and Bogdan Stefan Vasile<sup>1,\*</sup>

<sup>1</sup> National Research Center for Micro and Nanomaterials, Department of Science and Oxide Materials and Nanomaterials, Politehnica University of Bucharest, 060042 Bucharest, Romania; roxpopescu@yahoo.co.uk (R.C.P.); ecaterina.andronescu@upb.ro (E.A.)

<sup>2</sup> Department of Life and Environmental Physics, “Horia Hulubei” National Institute for Physics and Nuclear Engineering, 077125 Magurele, Romania

\* Correspondence: bogdan.vasile@upb.ro; Tel.: +40-727-589-960

Received: 31 October 2019; Accepted: 11 December 2019; Published: 16 December 2019



**Abstract:** Functionalization of nanomaterials can enhance and modulate their properties and behaviour, enabling characteristics suitable for medical applications. Magnetite (Fe<sub>3</sub>O<sub>4</sub>) nanoparticles are one of the most popular types of nanomaterials used in this field, and many technologies being already translated in clinical practice. This article makes a summary of the surface modification and functionalization approaches presented lately in the scientific literature for improving or modulating magnetite nanoparticles for their applications in nanomedicine.

**Keywords:** magnetite nanoparticles; Fe<sub>3</sub>O<sub>4</sub>; functionalization; surface modification; conjugation; nanomedicine; biocompatibility; clinical translation

## 1. Introduction

As a preponderance of biological processes begin and take place at molecular level, it is understandable why diagnosis and therapeutic solutions have been sought at the nanoscale. The use of nanoparticles in medicine is determined by the processes occurring at the bio-interface. In this context, manipulation of surface properties is highly important as it can determine the fate and functionality of the nano-system and can be achieved through the application of different surface functionalization.

During the last few years, magnetite (Fe<sub>3</sub>O<sub>4</sub>) nanoparticles have been attracting interest, especially in the area of clinical-oriented medical applications, many of which have already been approved by Food and Drug Administration (FDA), such as diagnosis [1,2], hyperthermia cancer treatment [3] or combating iron deficiencies [4]. This was possible due to their properties like biocompatibility [5–8], biodegradability [9–11], magnetic behaviour [12,13] and the possibility of easy functionalization [14,15]. Other possible uses of these nanoparticles might be in fields like catalysis [16,17], environmental remediation [18–20], electronics [21–23].

The route of synthesis enables controlling not only the chemical composition, but also the size, shape, surface properties and magnetic properties. The chemical methods for synthesis offer the advantage that the resulting nanoparticles can be functionalized at the end of the process, which ensures improved stability compared to non-functionalized materials and conservation of magnetic properties.

One of the most common and easiest chemical methods for magnetite nanoparticles synthesis is the co-precipitation developed by Massart in 1981 [24]. The method resides in the reaction between the ferric and ferrous ions in a basic medium. Different ferric and ferrous salts can be used as precursors (like chlorides, sulfates) and different bases, such as sodium hydroxide [25,26], ammonia [27,28]. The molar ratio of the precursor ions is usually 2:1 (Fe(III): Fe(II)), however, smaller ratios can be employed (such as 1.5:1), as the oxidation of Fe<sup>2+</sup> can occur [29] and the pH of the precipitation solution should

be kept between pH = 9–14 [26,30]. Also, a low concentration of O<sub>2</sub> is favorable, in order to prevent the oxidation of the nanoparticles and loss of magnetic properties [27]. A non-oxidant medium can be assured by the addition of nitrogen, in gas form or dissolved (such as in ammonia solution). Typically, the synthesis is undertaken in low-heat conditions (about 80 °C [31]), however, room temperature reactions can take place [32]. Moreover, the introduction of surfactants or other organic molecules in the reaction medium (the precipitation base) or in the precursor mixture, can influence the size, shape and surface properties of the resulting nanoparticles [33,34] through the formation of small micelles which limit the space of nucleation and growth available for the nanoparticle. Interactions between the organic phase and the terminal groups of the nanoparticles might be facilitated and in situ conjugations of the magnetite nanoparticles can take place [35].

The advantages of the co-precipitation method are rapidity, ease, reproducibility and high-yield synthesis, however, the main disadvantage is given by the fact that, in order to obtain a narrow size distribution of the resulting nanoparticles, some reaction parameters must be strictly assured [36]. Table 1 summarized how reaction parameters influence the properties of the resulting nanoparticles in the co-precipitation of the ferric and ferrous ions.

**Table 1.** Influence of reaction parameters on the properties of magnetite nanoparticles resulting from the co-precipitation method.

No.	Reaction Parameter	Property	Measure	Reference
1	Fe <sup>3+</sup> /Fe <sup>2+</sup> ratio	Iron oxide phase	Directly proportional	[37]
		Magnetism	Inversely proportional	[38,39]
		Dimension	Directly proportional	[39,40]
2	pH value	Iron oxide phase	Inversely proportional	[41]
		Magnetism	Inversely proportional	[38,42]
		Dimension	Insignificant	[42]
3	Type of base	Iron oxide phase	Depending on the type of base	[26]
		Magnetism	Depending on the type of base	[26]
		Dimension	Depending on the type of base	[26]
4	Temperature	Iron oxide phase	Directly proportional	[43]
		Magnetism	Inversely proportional	[44]
		Dimension	Inversely proportional	[40,45]
5	Concentration of precursors	Dimension	Directly proportional	[40]
6	pH of the precursor solution	Iron oxide phase		[40]
		Magnetism		[40]
		Dimension	Directly proportional	[40]
7	Addition of surfactants	Dimension	Directly proportional	[38,46,47]
		Surface charge	Dependent on the surfactant	[47]
		Composition	Dependent on the surfactant	[47]
		Shape	Dependent on the surfactant	[33]
		Magnetisation	Dependent of the surfactant	[47]

The solvothermal method is the second most popular method for the obtaining of magnetite nanoparticles and is performed in the presence of solvents, using temperatures that are higher than the boiling points of the solvents. The reaction is performed inside an enclosed system, like the autoclave, at high pressures. The composition of solvents influences the shape and size of the nanoparticles [48] however, the size is significantly determined by the temperature and duration of reactions. Different mixtures of agents such as tri ethylene glycol [49], oleylamine and ethylene glycol [50], or benzyl ether [51]. can be added in the solvent mixture in order to act as reducing agents for the precursor(s), leading to the synthesis of highly stable functionalized magnetite nanoparticles.

The hydrothermal method is based on the use of high temperatures and pressures to obtain single  $\text{Fe}_3\text{O}_4$  crystals [52]. Saturation of the precursors is required to initiate crystallization and this is enabled by a temperature difference between the precursors (crystallization area) and an aqueous area in the autoclave.

The microemulsion method uses micelles as nanoreactors for the nucleation and growth of magnetite nanoparticles in a limited space [53]. Thus, one main advantage of this method would be low polydispersity indices of the resulting nanoparticles and controlled morphology of these. Moreover, the nanoparticles are in situ functionalized through encapsulation [54,55].

Lately, a lot of non-conventional methods have been used in order to obtain magnetite nanoparticles. For example, the gas flame synthesis leads to highly dispersed nanoparticles with low polydispersity indices being obtained [56,57]; moreover in situ functionalization can be applied [58].

A rigorous control of the parameters of the synthesis method leads to crystalline nanoparticles with unique mineralogical phase composition being obtained. Magnetite nanoparticles have inverse spinel structure, with a face centred cubic lattice, where the iron ions are placed in the interstitial sites.

Moreover, a controlled synthesis assures and conserves the native properties of magnetite nanoparticles, such as the property of superparamagnetism, with high magnetic susceptibility, which in the absence of magnetic field shows null magnetization [59,60]. Temperature can randomly change the orientation of the magnetic spins, but this effect can also occur after a certain time (Neel relaxation time), due to the magnetic anisotropy of the nanoparticle. Placing  $\text{Fe}_3\text{O}_4$  nanoparticles in an exterior magnetic field causes the orientation of the nanoparticles magnetic moments with the magnetic field, while alternated magnetic fields repeatedly change the orientation of the magnetic moments, with an energy loss, converted to thermal energy. In order to preserve the magnetic property of  $\text{Fe}_3\text{O}_4$  nanoparticles, different functionalization approaches are employed.

The fate of magnetite nanoparticles in the human body is highly dependent on size, surface properties and terminal functional groups. It has been proved that the physical characteristics of the nanoparticles, such as size [61–63] and shape [64–67], influence their relationship with living cells. Additionally, surface properties [68,69], not only dictate the interaction with the biological barriers (membranes, vascular lumens), but can also modulate the way in which the nano-complex is perceived by the cells and tissues. In nanomedicine, this can dictate the effectiveness towards clinical translation. A rigorous control of the physical and chemical properties of magnetite nanoparticles can, most of the time, decide the fate of the nano-system and its ability to fulfil the requirements for which it has been designed and developed [70]. The route of administration can also determine the outcome of the nanoparticles, as they can encounter more or less biological barriers in their way to the targeted area.

Ma et al. [71] made a study on Kunming mice that were daily injected intraperitoneally during 1 week with different concentrations of  $\text{Fe}_3\text{O}_4$  nanoparticles (0, 5, 10, 20, 40 mg/kg), the subjects presenting lesions and the impairment of the hepatic and renal tissues, by means of oxidative mechanisms; the maximum recommended dose was 5 mg/kg. Wang et al. [72] determined the presence of  $\text{Fe}_3\text{O}_4$  nanoparticles in the brain after the intraperitoneal injection. Following intragastric administration of 600 mg/kg magnetite nanoparticles to mice [73], a maximum of concentration was determined in lungs and kidneys after 6 h of administration, in liver, brain, stomach and small intestine after 24 h, in heart and spleen after 3 days, respectively in peripheral blood after 5 days. Intravenous injection (15 mg/kg, 5 times) in C57BL/6 mice determined an accumulation of magnetite nanoparticles in liver, lungs and spleen, which were degraded to non-magnetic iron oxide species [74].

Due to the high surface-to-volume ratio, as a result of the nanometric dimension many hydroxyl terminal groups are available for conjugation with other molecules (Figure 1). It is this property that enables a lot of practicable approaches for surface modification, in order to alter and modulate the physical and chemical behaviour of magnetite nanoparticles. This review article discusses different approaches of functionalization for magnetite nanoparticles applications in medicine.

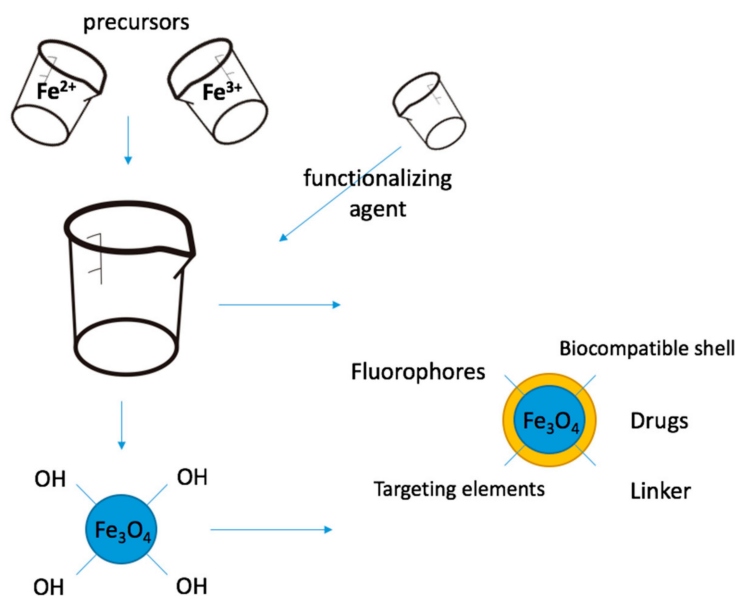


**Figure 1.** Schematic representation of the two main types of magnetite nanoparticle functionalization processes for medical applications: in situ, respectively, post-synthesis functionalization.

## 2. Functionalization of Magnetite Nanoparticles

Besides their advantages, magnetite nanoparticles have some major flaws, like rapid agglomeration, chemical reactivity, high surface energy, oxidation, which might alter their biocompatibility, properties and performance. In order to prevent these unwanted events, different surface functionalization is applied.

The functionalization refers to the conjugation of different molecules. In case of nanoparticles, this process determines a modification of the surface chemistry, which leads to changes in the physical, chemical and biological properties.

There are different types of functionalization. Depending on the time when it is done, the functionalization process can be in situ [75–77], in case the conjugation takes place simultaneously with the nucleation process of the nanoparticle, during the synthesis or post-synthesis [78,79], when the functionalization reaction(s) is (are) done after the synthesis of the nanoparticles (Figure 1).

By taking into consideration the chemistry of functionalization, either non-covalent or covalent bindings can take place between the surface modifying molecule and the magnetite nanoparticles. The non-covalent conjugation [80–82] mainly takes place through interactions that are based on the receptor-ligand affinity principle. Some examples are the electrostatic interactions, entrapment into secondary elements (like polymeric films) or  $\pi$ - $\pi$  stacking. In this case, mostly ionic bonds appear, following the transfer of one electron from a metallic to a non-metallic atom and the electrostatic interaction between the resulting ions.

In the case of covalent binding [83,84], different chemical reactions can take place during the functionalization process, such as substitution (nucleophile or electrophile), addition (nucleophile or electrophile), elimination, oxidation, reduction, polymerization, or esterification, in presence of different catalysts. In order to conjugate the desired molecule on the surface of the magnetite nanoparticles, intermediary linkers can be used, such as oleic acid [85], aminopropyltriethoxy silane [86], 3-(trimethoxysilyl) propyl methacrylate [87].

Sometimes, the preferred approach is to have a non-specific physical sorption, which would give a less stable conjugation (in case of delivery application or to facilitate the degradation of the nano-system), but chemical sorption can also be employed. In this case, covalent bonds can appear between identical atoms or different atoms which share electrons, each atom participating with one electron. This appears for non-metal elements. These are classified as non-polar covalent bonds

(between the same type of atoms), covalent bonds between different atoms, coordinative bonds (when two electrons are shared).

Metallic bonds are chemical bonds that form between metal elements. It is very rare that this interaction takes place between the Fe atoms in the oxide structure of magnetite and other metals, when developing core-shell metallic nanoparticles. For example, Han C.W. et al. [88] has obtained Fe<sub>3</sub>O<sub>4</sub>-Au core-shell nanoparticles by in situ vacuum annealing of dumbbell-like Au-Fe<sub>3</sub>O<sub>4</sub> nanoparticles obtained by epitaxial growth of magnetite on Au nanoparticles. The process was undertaken using a transmission electron microscope and recorded. During the annealing, the gold nanoparticles transformed into a gold nano-film, which was melting the surface of the magnetite nanoparticle, simultaneously with the reduction of the Fe<sub>3</sub>O<sub>4</sub> nanoparticle, taking place a strong metal-support bonding between the two components.

Different approaches of magnetite nanoparticles functionalization (Figure 1) will be discussed in the following sections, depending on the type of conjugation agent (inorganic or organic) and related to their biomedical applications.

### 3. Inorganic Functionalization of Magnetite Nanoparticles

#### 3.1. Oxides

Among oxides, SiO<sub>2</sub> (silica) coating is one of the most commonly used approaches for nanoparticle surface modification, especially in the case of iron oxides like magnetite. This is mainly determined by the properties induced by silica coating of Fe<sub>3</sub>O<sub>4</sub> nanoparticles, such as reducing the aggregation phenomena and thus improving the stability of the resulting functionalized nanoparticles [89], but also enhancing their biocompatibility [65,90].

There are several methods that can be used for SiO<sub>2</sub> conjugation on magnetite nanoparticles. The most frequently encountered approach is the sol-gel (Stoerber) method, which is based on the hydrolysis of tetraethoxysilane (TEOS) in an alcoholic medium, using ammonia as catalyst [91,92]. The method is popular due to its ease, but also due to the ability to obtain monodisperse-coated nanoparticles, with controlled dimension and shape. By using this approach, the chemical composition and structure, as well as magnetic properties of the Fe<sub>3</sub>O<sub>4</sub> nanoparticles, are preserved.

Another precise, but more elaborate method for the obtaining of Fe<sub>3</sub>O<sub>4</sub>@SiO<sub>2</sub> nanoparticles is the microemulsion method, which can be either water-in-oil (W/O) or oil-in-water (O/W). Such methods are usually employed for obtaining of Fe<sub>3</sub>O<sub>4</sub> nanoparticles and the in situ functionalization [93]. This method can also be microwave assisted [93,94].

Mesoporous silica, such as MCM-41 or SBA-15 have grown in interest due to their biocompatibility [95–97] and highly controlled porosity [98–100], which enable their use as controlled drug delivery platforms [101,102]. In order to obtain mesoporous silica-coated magnetite nanoparticles, a similar approach as in Fe<sub>3</sub>O<sub>4</sub>@ amorphous SiO<sub>2</sub> can be employed, but additionally an organic agent is used as template for the pore structure [103–105]. Such agents can be cetyltrimethylammonium bromide (CTAB), cetyltrimethylammonium chloride, n-octylamine, tetrapropylammonium bromide (TPABr) [106], triblock polymers like (EO)<sub>x</sub>-(PO)<sub>y</sub>-(EO)<sub>x</sub> (Pluronic L101, P103, P104, P105, F108) [107].

Due to their high porosity, the mesoporous silica-coated magnetite nanoparticles can absorb high quantities of therapeutic agents. Moreover, SiO<sub>2</sub> is dissolved in acidic environment, such as in the tumor microenvironment, inflammation, bacterial biofilm, or the endo-lysosomal compartments of the cells, making silica-functionalized Fe<sub>3</sub>O<sub>4</sub> great stimuli-responsive materials for the controlled delivery of therapeutic agents [108–110].

Other Si-based molecules have been used as functionalization agents for magnetite nanoparticles, in order to increase their stability or be used as linkers for further surface conjugation. Some examples are (3-aminopropyl)triethoxysilane (APTES) [111–113], 3-Aminopropyltrimethoxysilane (APTS) [114], (3-Mercaptopropyl)trimethoxysilane (MPTS) [115], triethoxy vinyl silane (VTES) [116],

aminosilane [117,118]. Table 2 summarizes some recent examples of Fe<sub>3</sub>O<sub>4</sub>@SiO<sub>2</sub> nano-systems and their applications in biomedicine.

**Table 2.** Recent approaches in Fe<sub>3</sub>O<sub>4</sub>-SiO<sub>2</sub> based nanostructures conjugates.

No.	System Description	Application	Type of Conjugation	Evaluation	Reference
1	Fe <sub>3</sub> O <sub>4</sub> @SiO <sub>2</sub>	Magnetic resonance imaging contrast substance as in vivo stem cell tracker	Negatively charged Fe <sub>3</sub> O <sub>4</sub> @citrate act as seeds for Si precursor; encapsulation using sol gel method;	Determination of distribution and chemical changes dynamics of Fe <sub>3</sub> O <sub>4</sub> @SiO <sub>2</sub> ; high chemical stability; distribution in cytoplasm;	[119]
2	Fe <sub>3</sub> O <sub>4</sub> @SiO <sub>2</sub> /anti-rHBsAg (Hepatitis B surface antigen)	Purification of recombinant Hepatitis B for vaccine production;	In situ functionalization; encapsulation using sol gel method;	In vitro isolation of rHBsAg antigen from <i>Pichia pastoris</i> yeast	[120]
3	Fe <sub>3</sub> O <sub>4</sub> @SiO <sub>2</sub>	Plasmid DNA purification	SiCl <sub>4</sub> cross-linker between Fe <sub>3</sub> O <sub>4</sub> @NH <sub>3</sub> and (3-aminopropyl)triethoxysilane (APTES); encapsulation using sol gel method;	Efficient in vitro plasmid DNA purification from <i>E. Coli</i> DH5a cells	[121]
4	Fe <sub>3</sub> O <sub>4</sub> @boronic acid/mesoporous (m) SiO <sub>2</sub>	Magnetic and pH triggered drug release;	–	Biocompatibility and high uptake in MC3T3-E1 cells; Controlled drug release and good magnetic properties;	[122]
5	Fe <sub>3</sub> O <sub>4</sub> @mSiO <sub>2</sub> /catalase (CAT)	Enzyme protection in catalysis;	Encapsulation in SiO <sub>2</sub> using TMOS (tetramethoxysilane) functionalization with APTES for CAT conjugation and growth of mSiO <sub>2</sub> using CTAB as template and TMOS;	Good stability and catalytic activity	[123]
6	Fe <sub>3</sub> O <sub>4</sub> @oleic acid@mSiO <sub>2</sub> /5-Fluorouracil	Drug delivery for cancer therapy;	In situ Fe <sub>3</sub> O <sub>4</sub> @oleic acid were functionalized with CTAB through weak interaction (Van der Waals); hydrolisation of tetraethoxysilane (TEOS) on Fe <sub>3</sub> O <sub>4</sub> /CTAB; encapsulation in mSiO <sub>2</sub> using the inversed microemulsion method;	In vitro biocompatibility for MCF-7 cells; efficient drug loading;	[124]

Numerous metal oxides have been used as functionalizing agents to modify the surface of magnetite nanoparticles, in order to obtain composites with improved functions. ZnO-conjugated Fe<sub>3</sub>O<sub>4</sub> nanoparticles have been developed in order to implement photocatalytic properties to the developed nano-systems. This phenomenon appears due to high oxygen vacancies on the surface of the nanoparticles and due to the fact that the electron-hole pairs induced by photon-triggering are inhibited by Fe<sup>3+</sup> ions [125]. Similar photocatalytic effects are given by Fe<sub>3</sub>O<sub>4</sub>@TiO<sub>2</sub> nanoparticles [102]. Shi L et al. [31] obtained Fe<sub>3</sub>O<sub>4</sub>@TiO<sub>2</sub> core-shell nanoparticles using post-synthesis functionalizing based on a hydrothermal approach. Similarly, Zhang L et al. [126] and Choi K-H et al. [127] used the solvothermal synthesis for microsphere preparation.

### 3.2. Metals

The surface conjugation of Fe<sub>3</sub>O<sub>4</sub> with different metals has been employed in order to improve the biocompatibility of magnetite nanoparticles and to induce an inert character to the final nano-structure. The metal coating of Fe<sub>3</sub>O<sub>4</sub> nanoparticle surface can be done either directly or through an intermediate functionalizing layer.



Core-shell magnetite@gold nanoparticles are interesting for their multifunctionality. The direct route to obtain this type of nano-composites is by directly reducing  $\text{Au}^{3+}$  ions on the surface of the  $\text{Fe}_3\text{O}_4$  nanoparticles, using reducing agents such as sodium citrate [60,128], sodium borohydride [129], and hydroxylamine hydrochloride [130]. Through this method mostly result dumbbell-like, core-satellite, or sometimes star-shaped structures, but core-shell nanoparticles can only result after multiple repetitions of the coating procedure. The main disadvantage of this method is the low yield synthesis, as many gold nanoparticles result [131]. Moreover, the reduction of  $\text{Au}^{3+}$  into  $\text{Au}^0$  takes place at the boiling point of the watery solution (80–90 °C), which might lead to an oxidation of  $\text{Fe}_3\text{O}_4$  and loss of magnetic properties.

Also, a more efficient direct method of conjugation might be in situ functionalization, through the organic synthesis approach [132]. Usually, these routes employ different agents to reduce  $\text{Fe}(\text{acac})_3$  [132] or  $\text{FeO}(\text{OH})$  [133] in presence of  $\text{HAuCl}_4$  which is simultaneously reduced, forming core-shell structures. Other organic molecules, such as oleic acid [134] are used to act as reducing and stabilization agents at the same time.

The use of an intermediary layer between the previously-synthesized magnetite nanoparticles and the gold layer acts as a “glue” between the two components. In situ or post-synthesis functionalization of iron oxide nanoparticles is undertaken, in order to obtain a functional layer that can either attract the  $\text{Au}^{3+}$  ions, which are afterwards reduced to  $\text{Au}^0$  using a third substance [135,136], or the conjugated molecules act as a reducing agent themselves [134].

$\text{Fe}_3\text{O}_4$ -Au conjugated nanoparticles have applications in medical imaging. Due to the presence and properties of both magnetite and gold phases, such nanoparticles can be used as a contrast substance in both magnetic resonance imaging (MRI), computer tomography (CT) and photoacoustic imaging (PA). For attempt, Hu Y et al. [137] developed  $\text{Fe}_3\text{O}_4@Au$  nano-systems starting from  $\text{Fe}_3\text{O}_4@Ag@$ citric acid as seeds for  $\text{Au}^{3+}$ . The resulting star-shaped nanoparticles were functionalized with polyethyleneimine (PEI) to improve stability and folic acid to induce the targeting ability (Figure 2). Ge Y et al. [138] used antibody (McAb) cetuximab (C225) conjugation of  $\text{Fe}_3\text{O}_4@Au$  to induce targeting ability for glioblastoma. The functionality of  $\text{Fe}_3\text{O}_4@Au$  nano-composites for targeted tumor imaging has been proved in vivo [137–139].

Other possible application of magnetite-gold nano-conjugates refers to their use in cancer radiotherapy, following their activation with different types of radiation: ionizing radiation (IR) [140,141], near-infrared (NIR) radiation [134,142] and radiofrequency (RF) [143] radiation. Radiotherapy mediated by nanoparticles has been considered as an approach that overcomes the resistance of tumor cells to radiotherapy and/or chemotherapy [144–147].

Generally, the use of metal elements to radiosensitize tumor cells is based on increasing the photoelectrical absorption, after their accumulation inside the malignant tissue. The high atomic number elements absorb most of the radiation compared to the surrounding healthy tissues and, due to the photoelectric and Compton effects, lower energy photons, Auger secondary electrons and low-energy secondary electrons are released [148–151]. Also, an enhanced production of reactive oxygen species occurs, due to the formation of secondary electrons and photons, but also due to the high surface reactivity of the nanoparticles [152,153]. This affects directly the DNA of the tumor cells. Moreover, nanoparticles can directly interact with the DNA, forming bonds or intercalating into the DNA chain [154,155]. The biological outcome is oxidative stress, cell-cycle disruption and DNA repair inhibition [148] in the tumor cells.

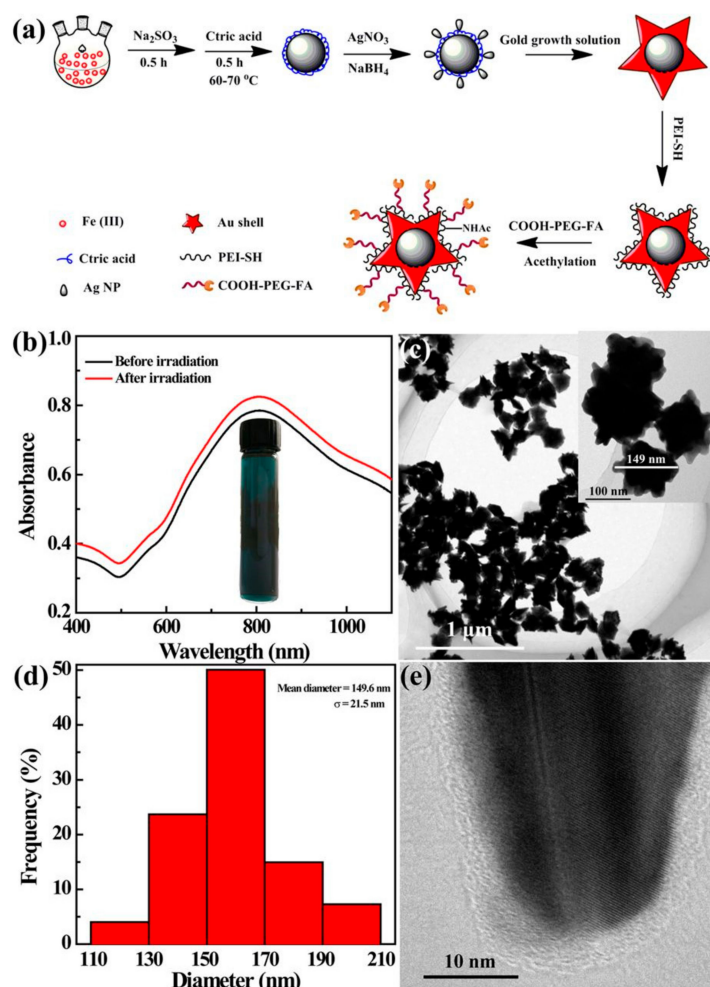


**Figure 2.** Star-shaped gold-conjugated  $\text{Fe}_3\text{O}_4$  nanoparticles; functionalization with organic molecules (polyethyleneimine, PEI): (a) schematic representation of the synthesis and conjugation processes; (b) ultraviolet–visible (UV–VIS) spectra for (non-) irradiated the nano-constructs; (c) transmission electron micrograph (TEM) of the resulted nanoconstructs; (d) histogram distribution of size; (e) high-resolution TEM (HR-TEM) of the resulted nanoconstructs; reprinted from [137].

The radiofrequency ablation (RFA) as a new method for cancer treatment has recently attracted more interest due to the fact that it does not harm normal tissues, when using frequencies from 10 kHz–900 MHz; the radiation has high penetration capability and non-ionizing effects on the tissues. The mechanism of toxicity upon cancer cells is produced by the induced thermal disruption determined due to the friction appearing in the ionic collisions of the biomolecules, when aligning in the alternating current flow [156]. RF-responsive nanomaterials have been proposed as probes for the treatment procedure, because of their ability to produce heat due to the resistance heating (in conductive materials, such as gold [153]), respectively magnetic heating (in magnetic materials, such as magnetite [157]). Gold-conjugated magnetite nanoparticles are excellent candidates for RFA treatment of cancer [142,158].

Another possible application of gold-conjugated magnetite nanoparticles is biosensing, due to the surface plasmon resonance property of gold [159–162]. Moreover, further functionalization of  $\text{Fe}_3\text{O}_4$ @gold with different antibodies gives the ability of specific targeting of cells, which together with the magnetic properties of the nano-systems enable their applicability in cell sorting or cell separation [163,164].

Platinum-conjugated magnetite nanoparticles also have possible applications in radiotherapy enhancement. Also an inert noble metal, Pt has an atomic number higher than Au, being able



to induce higher radiosensitizing effects [165,166]. Ma M. et al. [167] used a “glue” layer, DMSA (meso-2, 3-dimercaptosuccinic acid), for Pt ions that were reduced using NaBH<sub>4</sub> on the surface of previously-synthesized magnetite nanoparticles, in order to obtain dumbbell-like structures. A similar approach was employed by Wu D et al. [168] who used MnO<sub>2</sub> as intermediary layer for Pt ions absorption followed by reduction on the surface of the Fe<sub>3</sub>O<sub>4</sub>@MnO<sub>2</sub> nano-conjugate.

Silver coated magnetite nanoparticles can be obtained using the same approaches as gold-magnetite conjugates. Their applications in the medical field vary from catalysis [169], contrast substance in medical imaging [170,171], radiation therapy [172], the most frequent application being given by their anti-microbial properties [173]. Chang M et al. [174] obtained Fe<sub>3</sub>O<sub>4</sub>@Ag nanoparticles using in situ functionalization and proved their effect against *E. coli* strains. Brollo M. E et al. [175] synthesized brick-like nano-composites using a thermal decomposition method and in situ conjugation.

#### 4. Carbon-Based Functionalization of Magnetite Nanoparticles

The carbon-based functionalization of magnetite nanoparticles is treated separately from the (in)organic sections, as both inorganic (such as SiC [176]), as well as organic (graphene, carbon nanotubes) and Fe<sub>3</sub>O<sub>4</sub>@C composites are approached.

The majority of Fe<sub>3</sub>O<sub>4</sub>@C composites applications are in electronics (used as supercapacitors [177], anode materials in lithium-ion batteries [178], absorbents [177]). These materials can be obtained by in situ or post-synthesis functionalization, using the hydrothermal approach [179–181].

For applications in the biomedical field, the conjugation of magnetite nanoparticles and carbon-based nanostructures, such as graphene, carbon nanotubes or fullerenes are more often encountered. Amide bonding is a very frequent approach in conjugation of Fe<sub>3</sub>O<sub>4</sub> and carbon-based nanoparticles [158], alongside with click chemistry. These types of reactions are modular reactions like cycloadditions, nucleophilic ring-openings, carbon multiple bond additions and non-aldol carbonyl reactions [182]. The most common type in functionalizing carbon-based nanomaterials is Cu(I)-catalysed azide-alkyne 3+2 cycloaddition (CuAAC) [183]. Table 3 presents recent examples of Fe<sub>3</sub>O<sub>4</sub>-carbon nanoparticles conjugates.

**Table 3.** Recent approaches in Fe<sub>3</sub>O<sub>4</sub>-carbon-based nanostructures conjugates.

No.	System Description	Application	Type of Conjugation	Evaluation	Reference
1.	Fe <sub>3</sub> O <sub>4</sub> @APS-graphene/5-Fluorouracil	Drug-delivery systems for cancer treatment;	Amide bonding using 1-ethyl-3-(3-dimethylaminopropyl) carbodiimide	In vitro drug release at acidic pH; efficient in vitro internalizing in hepatocarcinoma HepG2 cells; biocompatibility of the carrier nanoparticles;	[184]
2.	Fe <sub>3</sub> O <sub>4</sub> @APTES/graphene oxide (GO)/doxorubicin	Drug-delivery systems and imaging diagnosis in cancer management;	Amide bonding using N-(3-Dimethylaminopropyl)-N'-ethylcarbodiimide hydrochloride (EDC)	In vitro low cytotoxicity compared to GO; superparamagnetic properties and 10.7 r2/r1 relaxivity; fluorescence in VIS; high doxorubicin loading and 2.5 fold higher efficiency; (Figure 3)	[185]
3.	Fe <sub>3</sub> O <sub>4</sub> @azide-sodium ascorbate-GO@ alkyne	Efficient absorbent and removal of dyes;	Click chemistry approach between the azide functional groups on the Fe <sub>3</sub> O <sub>4</sub> , sodium L-ascorbate and alkyne functional groups on GO;	Superparamagnetic properties; efficient absorbent and removal of dyes;	[186]
4.	Fe <sub>3</sub> O <sub>4</sub> @GO	Magnetic fluids;	Absorption;	Improvement of friction and wear performances with magnetic field;	[187]
5.	Polyvinyl alcohol (PVA)/ Fe <sub>3</sub> O <sub>4</sub> @ carbon nanotubes (CNTs)	Absorbent and dye removal; Anti-bacterial effects;	–	Optimal dye removal and anti-bacterial properties;	[188]

Table 3. Cont.

No.	System Description	Application	Type of Conjugation	Evaluation	Reference
6.	Fe <sub>3</sub> O <sub>4</sub> /multi walled CNTs/laser scribed graphene/chitosan/glassy carbon electrode	Detection of heavy metals	–	Electrode for the determination of Cd <sup>2+</sup> and Pb <sup>2+</sup> using square wave anodic stripping voltammetry; wide linear range; ultralow detection limit; excellent repeatability, reproducibility, stability;	[189]
7.	Single-walled CNTs-PEG-Fe <sub>3</sub> O <sub>4</sub> @ carbon quantum dots (CQD)/doxorubicin/sgc8c aptamer	Targeted photodynamic and photothermal ablation of tumor cells; controlled drug delivery; targeted imaging using fluorescence and magnetic resonance imaging (MRI)	Through polyethylene glycol (PEG) linker using amide bonding;	Near infrared triggered production of reactive oxygen species and heat; good imaging properties; good biocompatibility of the carrier and cellular internalization; high drug loading ability; selective accumulation at tumor site in human adenocarcinoma (HeLa) tumor-bearing mice intravenously injected with the system;	[190]
8.	GO-Chitosan/Fe <sub>3</sub> O <sub>4</sub> /glucose oxidase	Glucose biosensor and magnetic resonance imaging;	–	Good glucose biosensing ability;	[191]

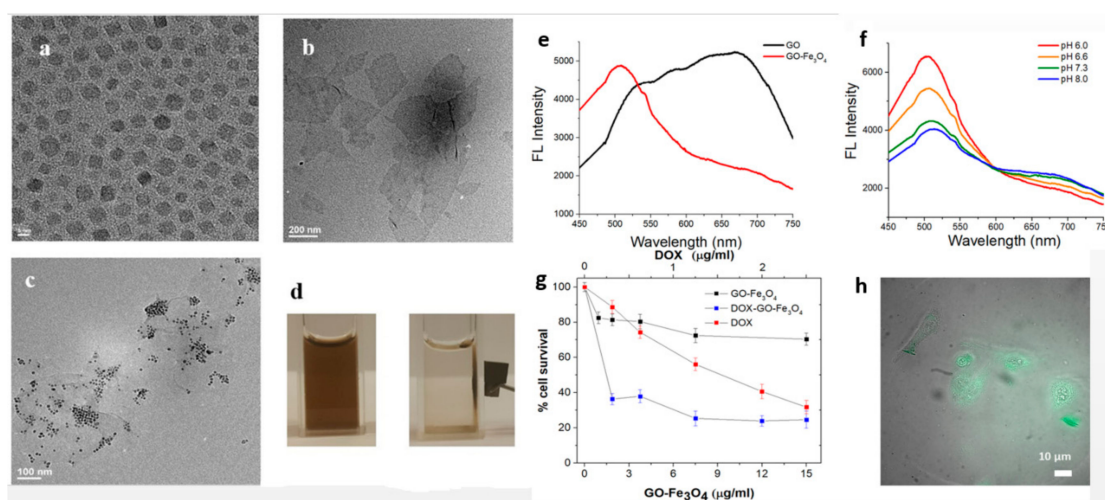


**Figure 3.** Fe<sub>3</sub>O<sub>4</sub>@(3-aminopropyl)triethoxysilane (APTES)-graphene oxide nano-system for drug delivery and diagnosis in cancer: (a) TEM of Fe<sub>3</sub>O<sub>4</sub> nanoparticles; (b) TEM of graphene oxide; (c) TEM of Fe<sub>3</sub>O<sub>4</sub>-graphene oxide conjugates; (d) magnetic manipulation of Fe<sub>3</sub>O<sub>4</sub>-graphene oxide conjugates in aqueous solution; (e) fluorescence spectra of graphene oxide and Fe<sub>3</sub>O<sub>4</sub>-graphene oxide conjugates; (f) fluorescence spectra of Fe<sub>3</sub>O<sub>4</sub>-graphene oxide conjugates at different pH; (g) HeLa cell survival (%) after incubation with equivalent concentrations of Fe<sub>3</sub>O<sub>4</sub>-graphene oxide conjugates, Fe<sub>3</sub>O<sub>4</sub>-graphene oxide conjugates loaded with doxorubicin, respectively doxorubicin; (h) fluorescence image of internalized Fe<sub>3</sub>O<sub>4</sub>-graphene oxide conjugates in HeLa cells; adapted from [185].

## 5. Organic Functionalization of Magnetite Nanoparticles

The functionalization of magnetite nanoparticles with organic compounds is mostly done in order to improve their stability [192] and biocompatibility [193]. Another reason would be to improve their interaction with biological barriers (cellular membranes, vascular endothelium, blood-brain barrier) and facilitate the nanoparticles' passage through these [194,195].

Furthermore, magnetite nanoparticles have a hydrophobic character which favours the adsorption of serum proteins, causing not only blood clogging, but also leading to the opsonisation phenomenon. Through this, the nanoparticles are immediately collected by the cells of the mononuclear phagocyte system and eliminated from systemic circulation. In order to improve the pharmacological kinetics of the magnetite nanoparticles, functionalization with hydrophilic polymers, such as polyethylene glycol (PEG) [196] is applied.

In case of controlled delivery of therapeutic substances, organic materials and especially polymers are the best stimuli-responsive materials (responsive to changes in temperature, pH, light).  $\text{Fe}_3\text{O}_4$  nanoparticles functionalized with biocompatible responsive polymers are ideal for such applications, as the magnetite core enables magnetic targeting properties of the system, while the soft shell encapsulates large quantities of drug molecules.

Also, polymers enable many available functional groups for the conjugation of other molecules. Thus, specific molecules can be conjugated for targeting certain type of cells or area of the body (like folic acid [197,198], L-3,4- dihydroxyphenylalanine (L-DOPA) [199], riboflavin [200], arginine-glycine-aspartate (RGD) [201] for cancer targeting) and/or light-responsive molecules for detection and imaging (such as fluorescein isotiocyanate-FITC [202]). Moreover,  $\text{Fe}_3\text{O}_4$  can be used as contrast substance in MRI because of its ability to alter the spin-spin relaxation time T2 of the surrounding water protons [203]. Given all these properties, functionalized magnetite nanoparticles can be used as multifunctional platforms for cancer detection and therapy.

Organic materials for magnetite nanoparticles functionalization will be discussed in separate sections as follows: small molecules and surfactants, lipids, polymers, phytochemicals, respectively drug molecules.

### 5.1. Small Molecules and Surfactants

Functionalization of magnetite nanoparticles with amphiphilic molecules (surfactants) has been proved as a good solution to improve the stability of the suspensions [204,205]. However, surfactants can rather have a toxic behaviour and are not recommended for biological applications [206–208].

Instead, functionalization with small molecules was proposed. Oleic acid is the most common small lipophilic molecules used for the functionalization of magnetite nanoparticles.  $\text{Fe}_3\text{O}_4$ @oleic acid has good stability [209], biocompatibility [210] and can be used for further functionalization: oleic acid can act either as a "glue" layer to conjugate other compounds [211] or as a starting point in ligand exchange approach [212,213].

Functionalization of magnetite nanoparticles with small molecules or surfactants is mostly done in situ using solvothermal [51,214,215] or microemulsion [53,216] approaches, however, post-synthesis conjugation can also be done [217,218].

Figure 4 [219] illustrates an approach for oleic acid capping of magnetite nanoparticles and the morphological and hydrodynamic properties of the resulting functionalized nanoparticles, in comparison with bare  $\text{Fe}_3\text{O}_4$ .

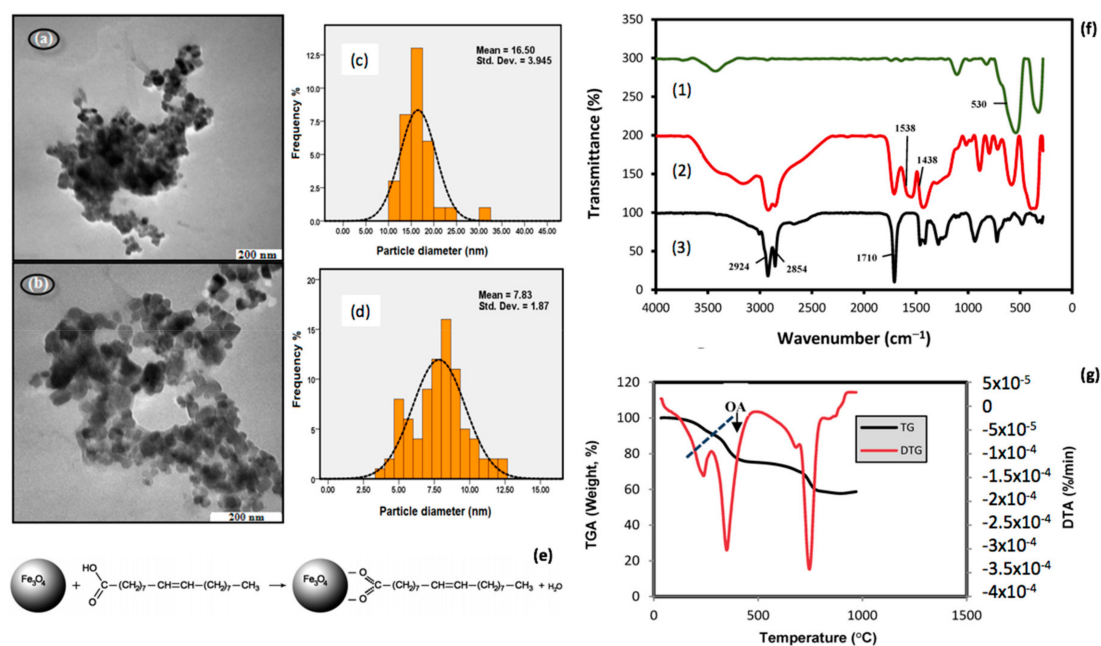


**Figure 4.** Surface conjugation of magnetite nanoparticles with oleic acid: transmission electron microscopy (TEM) image for (a) bare  $\text{Fe}_3\text{O}_4$ , respectively (b) oleic acid conjugated  $\text{Fe}_3\text{O}_4$ ; particle diameter distribution for (c) bare  $\text{Fe}_3\text{O}_4$ , respectively (d) oleic acid conjugated  $\text{Fe}_3\text{O}_4$ ; (e) schematic representation of the capping principle; (f) Fourier transform infrared (FTIR) spectra of  $\text{Fe}_3\text{O}_4$  (1)  $\text{Fe}_3\text{O}_4$ /oleic acid (2), respectively oleic acid (3); (g) thermogravimetric analysis (TGA) and differential thermogravimetric analysis (DTA) curves for oleic acid conjugated  $\text{Fe}_3\text{O}_4$ ; adapted from [219].

## 5.2. Lipids

Lipids are the main component of cellular membranes, thus conjugation with magnetite nanoparticles would be ideal for biomedical applications. Lipid-coated nanoparticles favour the interaction with and passage through biological membranes [220,221], enhancing the biocompatibility of  $\text{Fe}_3\text{O}_4$  nanoparticles [197,222] and preventing the opsonisation phenomenon [223]. The obtaining of lipid-conjugated magnetite nanoparticles is most of the time done through encapsulation [224,225].

## 5.3. Polymers

The functionalization of magnetite nanoparticles with polymers can be undertaken using both in situ and post-synthesis functionalizing. It is very common in case of co-precipitation method for  $\text{Fe}_3\text{O}_4$  synthesis to introduce polymer molecules in the precipitation solution, in order to determine the simultaneous functionalization, nucleation and growth of the nanoparticles [226,227]. In this case, mostly non-covalent bonds (electrostatic forces) appear between the polymers and magnetite nanoparticles.

The latter method starts from previously synthesized magnetite nanoparticles that can be conjugated with different polymers through the available hydroxyl groups on their surface. These are mostly condensation reactions. One approach is through the ester bond formation. Also, intermediate linkers can be used, such as APTES, which enable amine terminal groups on the surface of the magnetite nanoparticles. These can be then coupled with different polymers through an amide bond formation.

The main reason for polymer surface functionalization of magnetite nanoparticles is the increase of stability, as the polymeric molecules act as splicing agents between the magnetic nanoparticles, preventing their aggregation. The longer the polymeric chain, the higher the stability of the nanoparticles. However, this can produce an inverse effect, as a reduced magnetic response can occur when stimulating the functionalized nanoparticles with an exterior magnetic field.

Polyethylene glycol (PEG) is the most widely used polymer for magnetite nanoparticles functionalization. PEG with different molecular weights are employed, in order to modulate the hydrodynamic properties of the resulting nano-composites and to improve their stability [228,229]. Other frequently used polymers for Fe<sub>3</sub>O<sub>4</sub> nanoparticles functionalization are polyethyleneimine (PEI) [230,231], glucose [232–234], dextran [235,236], and chitosan [237–239]. Table 4 summarizes some examples of polymer-functionalized magnetite nanoparticles and their applications.

**Table 4.** Recent approaches in Fe<sub>3</sub>O<sub>4</sub>-polymer-based nanostructures conjugates.

No.	System Description	Application	Type of Conjugation	Evaluation	Reference
1.	Fe <sub>3</sub> O <sub>4</sub> @ poly(polyethylene glycol methacrylate-co-acrylic acid) (P(PEGMA-AA))	Hyperthermia and MRI contrast substance;	Electrostatic interactions between the acrylic acid and positively-charged Fe <sub>3</sub> O <sub>4</sub> ;	Improved stability and salt tolerance; excellent blood compatibility; formation of blood protein corona; resistance to cell internalization; improvement of contrast in MRI;	[240,241]
2.	Fe <sub>3</sub> O <sub>4</sub> /methyl methacrylate/ethylene glycol dimethacrylate/hydroxyl ethyl methacrylate/gemcitabine	Hyperthermia and drug delivery for cancer therapy	–	Good incorporation of drug; temperature triggered release; (Figure 5)	[242]
3.	Fe <sub>3</sub> O <sub>4</sub> @PEG/Doxorubicin	Drug delivery and hyperthermia in cancer treatment;	In situ conjugation	pH responsive release of drug; no cytotoxicity of Fe <sub>3</sub> O <sub>4</sub> @PEG for human fibroblasts; Fe <sub>3</sub> O <sub>4</sub> @PEG/Doxorubicin showed good internalization and cytotoxicity for mouse skin fibrosarcoma; good magnetic properties;	[243]
4.	Fe <sub>3</sub> O <sub>4</sub> @ poly(lactic-co-glycolic acid) (PLGA)-PEG@ folic acid/curcumin	Targeted drug delivery for cancer treatment;	Encapsulation;	High drug loading and delivery; high in vitro targeting efficiency for cervical carcinoma; in vitro induction of apoptosis and reduction of tumor cell proliferation;	[244]
5.	Fe <sub>3</sub> O <sub>4</sub> @ C/carboxymethyl cellulose/chitosan/diclofenac sodium	Controlled drug delivery;	In situ conjugation and subsequent electrostatic conjugation;	High drug-loading efficiency; pH sensitive drug delivery;	[245]
6.	Fe <sub>3</sub> O <sub>4</sub> @ dextran	–	Covalent binding via electron pairing;	–	[246]
7.	Fe <sub>3</sub> O <sub>4</sub> @dextran	Near-infrared (NIR) photothermal ablation of tumor cells;	In situ encapsulation;	In vitro biocompatibility; in vitro and in vivo tumor growth inhibition after NIR activation;	[247]
8.	Fe <sub>3</sub> O <sub>4</sub> @ poly ε acrylic acid-gelatin/ hydroxyapatite/ polycaprolactone	Bone tissue engineering scaffolds for hyperthermia cancer treatment;	Electrostatic interactions between the acrylic acid and positively-charged Fe <sub>3</sub> O <sub>4</sub> ;	Characterisation of the magnetic behaviour for hyperthermia applications;	[248]



Table 4. Cont.

No.	System Description	Application	Type of Conjugation	Evaluation	Reference
9.	Fe <sub>3</sub> O <sub>4</sub> /poly-L-lactide (PLLA) nanofibers	Bone tissue engineering;	–	In vivo evaluation on tibia defect rabbit model; computer tomography and histological investigations revealed higher bone-healing potential than conventional PLLA	[249]

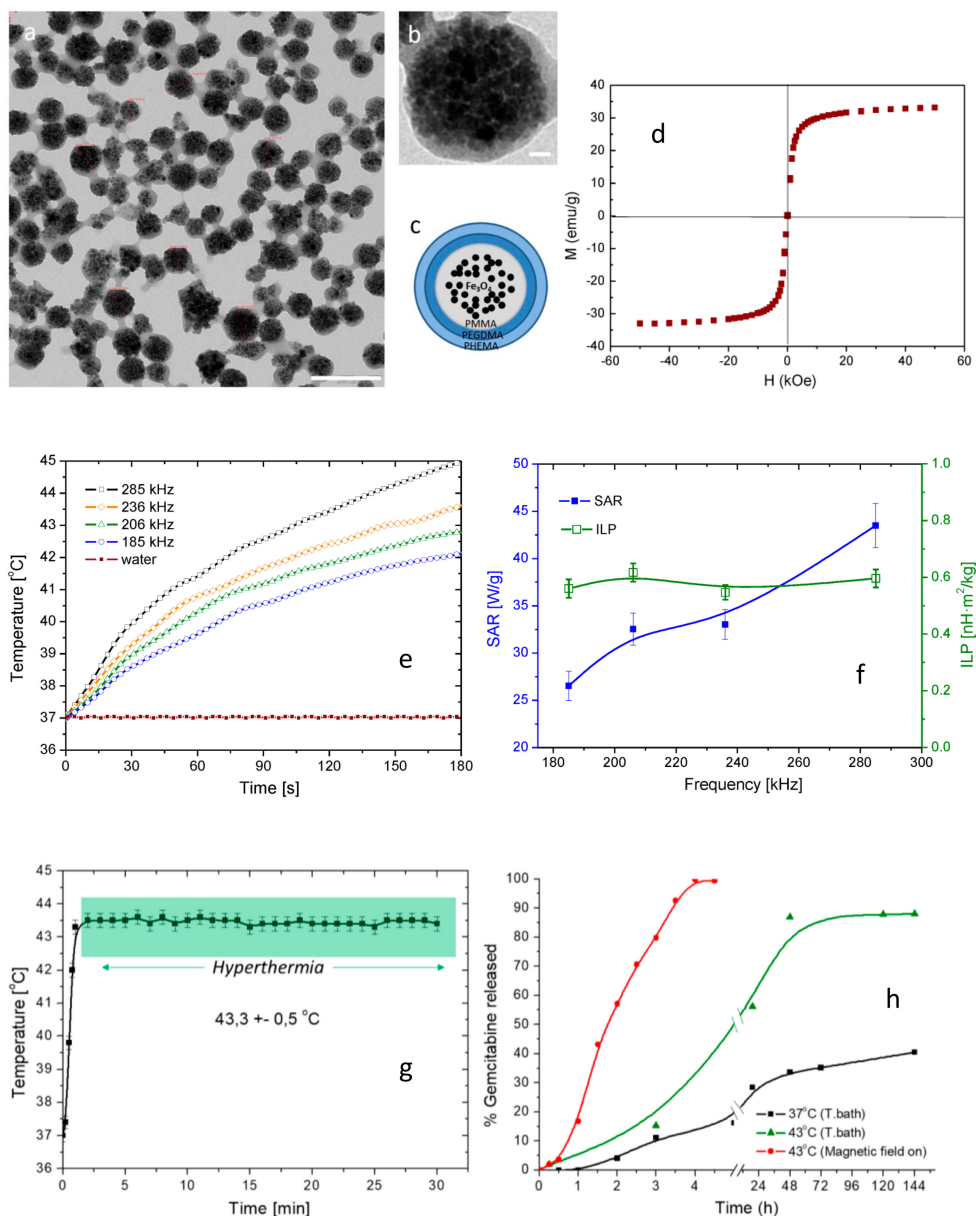


**Figure 5.** MagP-OH particles: (a) TEM image, scale 200 nm, (b) TEM detail, scale 20 nm, (c) schematic representation of MagP, (d) magnetisation curve of MagP, (e) time evolution of temperature for various frequencies, (f) Specific Absorption Rate (SAR) and Intrinsic Loss Power (ILP) for Ha = 16.2 kA/m, (g) hyperthermia measurement, (h) drug release measurement; adapted from [242].

Maier-Hauff K. group has studied the effects of soft polymer coated  $\text{Fe}_3\text{O}_4$  nanoparticle-mediated hyperthermia combined with external beam radiotherapy on glioblastoma multiforme patients [250–252]. Nowadays, this treatment plan has been clinically approved and used by MagForce [3].

Hyperthermia is a therapeutic procedure for cancer which rises the temperature of the tissue to about 41–45 °C for a certain period of time [253]. Tumor cells are sensitive to these temperatures, while normal healthy cells endure temperatures up to 46–47 °C. Nanoparticle-mediated magnetic hyperthermia uses the magnetic property of  $\text{Fe}_3\text{O}_4$  nanoparticles to produce thermal energy [254]. The nanoparticles are exposed to external alternated magnetic fields which cause successive (de) magnetization, the supplementary energy to reach the relaxation state being converted to thermal energy [255].

#### 5.4. Phytochemicals

Phytochemicals are chemical products derived from plants, which might have beneficial effects on human health. Conjugation of magnetite nanoparticles with different phytochemicals was done in order to improve their biocompatibility [256,257] and induce certain therapeutic properties (antibacterial [32,258–260], anticancer [11,261]). Mostly, these plant-originated chemicals are used as reducing agents for the iron precursors [262,263] during the synthesis of the nanoparticles. This process enables an in situ functionalization of the resulting materials with molecules in the plant extracts, which are mostly rich in hydroxyl groups. However, post-synthesis functionalization can also be employed [256].

In traditional medicine, phytochemicals have been used extensively due to their potential therapeutic activity, continuing to be the basis of alternative therapeutic approaches even today, in cancer therapy [264,265], anti-microbial applications [258,266], anti-inflammatory approaches [267,268], anti-viral and immune system enhancement [269]. Moreover, folic acid has been used extensively as targeting agent for tumour cells [270,271], as these cells exhibit a higher density of folic acid receptors on the membrane, compared to healthy cells.

In the case of anti-bacterial applications, one important branch refers to combating the medical devices associated infections and biofilm formation, one approach for preventing antibiotic resistant bacteria contamination being the use of alternative medicine. Figure 6 illustrates the compositional structure and biological characterisation of matrix-assisted pulsed laser evaporation (MAPLE) deposited  $\text{Fe}_3\text{O}_4@Cinnamomum\ verum$  thin films. These have been developed in the idea of implant surface modification with anti-bacterial potential. Such substrates are biocompatible for eukaryote cells (in the surrounding tissues) and exhibit a toxic effect against prokaryote (bacterial) cells.

#### 5.5. Drug Molecules

Magnetite-based nano-systems have been broadly used as drug-delivery systems [272–275]. A direct conjugation of the drug with the functional groups of magnetite is mostly undertaken in order to assure a targeted transport of the therapeutic molecules at the site of action through magnetic directing. Weak bonding (such as non-covalent interactions) between the two components is preferred, in order to allow facile delivery of the drug. Strong interactions may affect the chemical structure of the drug molecule and determine therapeutic properties loss.

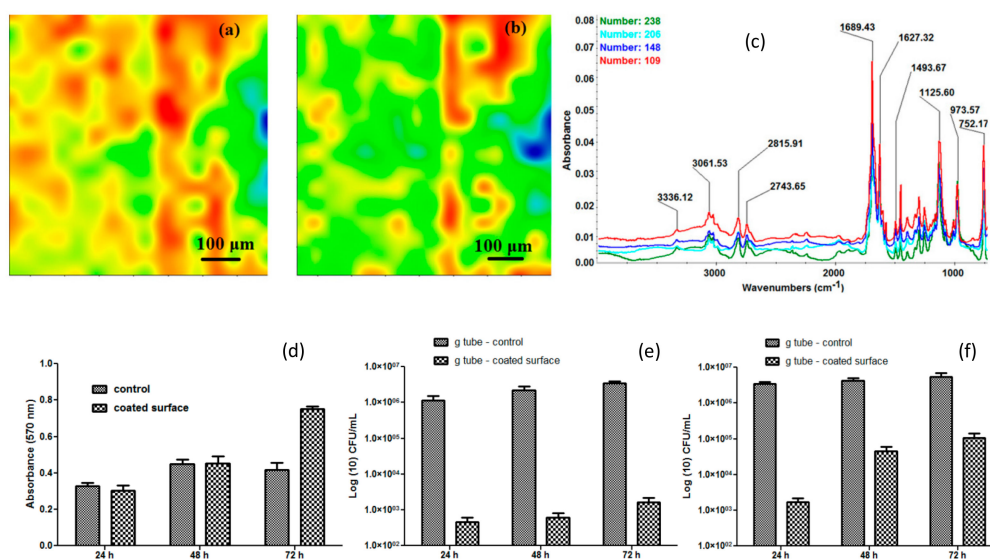


**Figure 6.** Matrix-assisted pulsed laser evaporation (MAPLE)-deposited  $\text{Fe}_3\text{O}_4@Cinnamomum\ verum$  at fluence  $F = 400\text{ mJ/cm}^2$ : Infrared microscopy-distribution of intensity of (a)  $2815\text{ cm}^{-1}$ , (b)  $1689\text{ cm}^{-1}$ , (c) IR spectra; (d) biocompatibility evaluation for endothelial cells; antibacterial evaluation—*S. aureus* biofilm formation (e), respectively, *E. coli* biofilm formation (f) [32].

## 6. Conclusions

In the context of the advancement of magnetite nanoparticles implications in nanomedicine, a high control of their hydrodynamic and biocompatibility properties should be guaranteed, besides the fulfilment of their main biomedical function. This can be assured through the conjugation of secondary components. This review summarizes the latest advances in various approaches for  $\text{Fe}_3\text{O}_4$  nanoparticles functionalization for nanomedicine applications:

- Multifunctionality of  $\text{Fe}_3\text{O}_4$  nanoparticles is given by its properties (magnetism, biocompatibility);
- They have many applications in the medical field, among which a few have been approved by the FDA for clinical use (MRI contrast substance, magnetic hyperthermia, iron deficiency supplement);
- The route of synthesis also determines the surface functionality among other properties;
- Surface functionalization determines an alteration of the surface chemistry, leading to changes in the physical, chemical and biological properties;
- Classification of functionalization processes. Depending on: time of functionalization (in situ, respectively post synthesis), chemistry of functionalization (non-covalent and covalent), chemistry of the functionalizing agent (inorganic and organic);
- Non-specific physical sorption is preferred in applications such as drug delivery systems;
- Among the oxides,  $\text{SiO}_2$  coating of magnetite nanoparticles is the most common because it enhances the biocompatibility and stability of the nanoparticles; some common approaches to obtain this conjugation are the sol-gel method, respectively, microemulsion;
- The mesoporous silica coating is biocompatible and offers high controlled porosity; is good for drug delivery applications;
- Metal oxide ( $\text{ZnO}$ ,  $\text{TiO}_2$ ) functionalization has photocatalytic applications;
- Surface functionalization of magnetite nanoparticles with metals induces an inert character; the most popular approach in this category is the conjugation of  $\text{Fe}_3\text{O}_4$  with gold because of its biocompatibility and multifunctionality; approaches to obtain this type of nanoparticles are: reduction of gold ions on the surface of magnetite nanoparticles, respectively, the organic synthesis approach; the final applications are numerous: medical imaging (MRI, CT, PA), radiosensitiation, radiofrequency ablation, biosensing, cell sorting;

- Carbon-Fe<sub>3</sub>O<sub>4</sub> nano-composites mostly have applications in electronics, but also in biosensing and drug delivery systems; in order to obtain these materials, the direct precipitation of magnetite nanoparticles on the surface of the carbon nanomaterial can be applied or a hydrothermal approach for in situ functionalization;
- The conjugation of magnetite nanoparticles with organic molecules has the advantage of improving the stability, biocompatibility and interaction with biological membranes of the Fe<sub>3</sub>O<sub>4</sub>; mostly has applications in the development of drug delivery systems;
- Surfactants have been used to improve the stability of the magnetite nano-constructs, but can have toxic effects;
- Lipid-encapsulated nanoparticles enhance the biocompatibility of the magnetite nanoparticles and improve their interaction with biological membranes, while preventing opsonisation;
- The functionalization of Fe<sub>3</sub>O<sub>4</sub> with polymers is the type of surface modification most encountered for these nanoparticles and can be undertaken both in situ (through electrostatic interactions) or post-synthesis (through condensation); it increases the stability and biocompatibility of magnetite nanoparticles, leading to applications in medical imaging, hyperthermia treatment of cancer, drug delivery systems, tissue engineering;
- A polymer-coated Fe<sub>3</sub>O<sub>4</sub> nanoparticle (MagForce) has been approved by the FDA for use in hyperthermia treatment of cancer;
- Drug-delivery systems based on magnetite nanoparticles can be developed for commercial medicines or phytochemicals; the therapeutic molecule can be directly conjugated on the Fe<sub>3</sub>O<sub>4</sub> surface or can be attached through an intermediate layer;
- Phytochemicals-Fe<sub>3</sub>O<sub>4</sub> are popular alternative medicines with antimicrobial, antitumor, anti-inflammatory or antiviral applications; conjugation with magnetite nanoparticles can be undertaken through both weak and strong interactions;
- Conventional drugs are mostly attached through strong interactions from the magnetite nanoparticles.

**Author Contributions:** The authors contributions are as follows: writing—original draft preparation, R.C.P.; writing—review and editing, B.S.V., R.C.P.; visualization, B.S.V., E.A.; supervision, E.A.

**Funding:** This research was funded by Operational Programme Human Capital of the Ministry of European Funds through the Financial Agreement 51668/09.07.2019, SMIS code 124705.

**Conflicts of Interest:** The authors declare no conflict of interest.

## References

1. Amag Pharmaceuticals. Available online: <http://www.amagpharma.com/our-products/> (accessed on 19 November 2019).
2. Wáng, Y.X.J.; Idée, J.M. A comprehensive literatures update of clinical researches of superparamagnetic resonance iron oxide nanoparticles for magnetic resonance imaging. *Quant. Imaging Med. Surg.* **2017**, *7*, 88–122. [[CrossRef](#)] [[PubMed](#)]
3. MagForce. Fighting Cancer with Nanomedicine. Available online: <http://www.magforce.de/en/home.html> (accessed on 7 October 2019).
4. Feraheme Ferumoxytol Injection. Available online: <https://www.feraheme.com> (accessed on 19 November 2019).
5. Zhang, D.; Du, Y. The Biocompatibility Study of Fe<sub>3</sub>O<sub>4</sub> Magnetic Nanoparticles Used in Tumor Hyperthermia. In Proceedings of the 2006 1st IEEE International Conference on Nano/Micro Engineered and Molecular Systems, Zhuhai, China, 18–21 January 2006; pp. 339–342. [[CrossRef](#)]
6. Chen, D.; Tang, Q.; Li, X.; Zhou, X.; Zhang, J.; Xue, W.-Q.; Xiang, J.-Y.; Guo, C.-Q. Biocompatibility of magnetic Fe<sub>3</sub>O<sub>4</sub> nanoparticles and their cytotoxic effect on MCF-7 cells. *Int. J. Nanomed.* **2012**, *7*, 4973–4982. [[CrossRef](#)] [[PubMed](#)]

7. Sun, J.; Zhou, S.; Hou, P.; Yang, Y.; Weng, J.; Li, X.; Li, M. Synthesis and characterization of biocompatible Fe<sub>3</sub>O<sub>4</sub> nanoparticles. *J. Biomed. Mater. Res.* **2007**, *80A*, 333–341. [[CrossRef](#)] [[PubMed](#)]
8. Tian, Q.; Ning, W.; Wang, W.; Yuan, X.; Bai, Z. Synthesis of size-controllable Fe<sub>3</sub>O<sub>4</sub> magnetic submicroparticles and its biocompatible evaluation in vitro. *J. Cent. South Univ.* **2016**, *23*, 2784–2791. [[CrossRef](#)]
9. Tseng, W.-K.; Chieh, J.-J.; Yang, Y.-F.; Chiang, C.-K.; Chen, Y.-L.; Yang, S.Y.; Horng, H.-E.; Yang, H.-C.; Wu, C.-C. A Noninvasive Method to Determine the Fate of Fe<sub>3</sub>O<sub>4</sub> Nanoparticles following Intravenous Injection Using Scanning SQUID Biosusceptometry. *PLoS ONE* **2012**, *7*, e48510. [[CrossRef](#)]
10. Gu, L.; Fang, R.H.; Sailor, M.J.; Park, J.H. In vivo clearance and toxicity of monodisperse iron oxide nanocrystals. *ACS Nano* **2012**, *6*, 4947–4954. [[CrossRef](#)]
11. Yew, Y.P.; Shameli, K.; Miyake, M.; Khairudin, N.B.B.A.; Mohamad, S.E.B.; Naiki, T.; Lee, K.X. Green biosynthesis of superparamagnetic magnetite Fe<sub>3</sub>O<sub>4</sub> nanoparticles and biomedical applications in targeted anticancer drug delivery system: A review. *Arab. J. Chem.* **2018**, 1–22. [[CrossRef](#)]
12. Patsula, V.; Moskvina, M.; Dutz, S.; Horák, D. Size-dependent magnetic properties of iron oxide nanoparticles. *J. Phys. Chem. Solids* **2016**, *88*, 24–30. [[CrossRef](#)]
13. Li, Q.; Kartikowati, C.W.; Horie, S.; Ogi, T.; Iwaki, T.; Okuyama, K. Correlation between particle size/domain structure and magnetic properties of highly crystalline Fe<sub>3</sub>O<sub>4</sub> nanoparticles. *Sci. Rep.* **2017**, *7*, 9894. [[CrossRef](#)]
14. Darwish, M.S.A.; Nguyen, N.H.A.; Ševců, A.; Stibor, I. Functionalized Magnetic Nanoparticles and Their Effect on Escherichia coli and Staphylococcus aureus. *J. Nanomater.* **2015**, *2015*, 416012–416022. [[CrossRef](#)]
15. Wu, W.; He, Q.; Jiang, C. Magnetic Iron Oxide Nanoparticles: Synthesis and Surface Functionalization Strategies. *Nanoscale Res. Lett.* **2008**, *3*, 397–415. [[CrossRef](#)] [[PubMed](#)]
16. Li, Z.-X.; Luo, D.; Li, M.-M.; Xing, X.-F.; Ma, Z.-Z.; Xu, H. Recyclable Fe<sub>3</sub>O<sub>4</sub> Nanoparticles Catalysts for Aza-Michael Addition of Acryl Amides by Magnetic Field. *Catalysts* **2017**, *7*, 219. [[CrossRef](#)]
17. Alishiri, T.; Oskooei, H.A.; Heravi, M.M. Fe<sub>3</sub>O<sub>4</sub> Nanoparticles as an Efficient and Magnetically Recoverable Catalyst for the Synthesis of  $\alpha,\beta$ -Unsaturated Heterocyclic and Cyclic Ketones under Solvent-Free Conditions. *Synth. Commun.* **2013**, *43*, 3357–3362. [[CrossRef](#)]
18. Araújo, R.; Castro, A.C.M.; Fiúza, A. The Use of Nanoparticles in Soil and Water Remediation Processes. *Mater. Today Proc.* **2015**, *2*, 315–320. [[CrossRef](#)]
19. Jiang, B.; Lian, L.; Xing, Y.; Zhang, N.; Chen, Y.; Lu, P.; Zhang, D. Advances of magnetic nanoparticles in environmental application: Environmental remediation and (bio)sensors as case studies. *Environ. Sci. Pollut. Res.* **2018**, *25*, 30863–30879. [[CrossRef](#)]
20. Gutierrez, A.M.; Dziubla, T.D.; Hilt, J.Z. Recent advances on iron oxide magnetic nanoparticles as sorbents of organic pollutants in water and wastewater treatment. *Rev. Environ. Health* **2017**, *32*, 111–117. [[CrossRef](#)]
21. De Teresa, J.M.; Fernández-Pacheco, A.; Morellon, L.; Orna, J.; Pardo, J.A.; Serrate, D.; Algarabel, P.A.; Ibarra, M.R. Magnetotransport properties of Fe<sub>3</sub>O<sub>4</sub> thin films for applications in spin electronics. *Microelectron. Eng.* **2007**, *84*, 1660–1664. [[CrossRef](#)]
22. Guo, L.; Sun, H.; Qin, C.; Li, W.; Wang, F.; Song, W.; Du, J.; Zhong, F.; Ding, Y. Flexible Fe<sub>3</sub>O<sub>4</sub> nanoparticles/N-doped carbon nanofibers hybrid film as binder-free anode materials for lithium-ion batteries. *Appl. Sur. Sci.* **2018**, *459*, 263–270. [[CrossRef](#)]
23. Salimi, P.; Norouzi, O.; Pourhosseini, S.E.M. Two-step synthesis of nanohusk Fe<sub>3</sub>O<sub>4</sub> embedded in 3D network pyrolytic marine biochar for a new generation of anode materials for Lithium-Ion batteries. *J. Alloys Compd.* **2019**, *786*, 930–937. [[CrossRef](#)]
24. Massart, R. Preparation of aqueous magnetic liquids in alkaline and acidic media. *IEEE Trans. Magn.* **1981**, *17*, 1247–1248. [[CrossRef](#)]
25. Kalantari, K.; Ahmad, M.B.; Shameli, K.; Bin Hussein, M.Z.; Khandanlou, R.; Khanehzaei, H. Size-Controlled Synthesis of Fe<sub>3</sub>O<sub>4</sub> Magnetic Nanoparticles in the Layers of Montmorillonite. *J. Nanomater.* **2014**, *2014*, 739485–739494. [[CrossRef](#)]
26. Mascolo, M.C.; Pei, Y.; Ring, T.A. Room Temperature Co-Precipitation Synthesis of Magnetite Nanoparticles in a Large pH Window with Different Bases. *Materials* **2013**, *6*, 5549–5567. [[CrossRef](#)] [[PubMed](#)]
27. Mo, Z.; Zhang, C.; Guo, R.; Meng, S.; Zhang, J. Synthesis of Fe<sub>3</sub>O<sub>4</sub> Nanoparticles Using Controlled Ammonia Vapor Diffusion under Ultrasonic Irradiation. *Ind. Eng. Chem. Res.* **2011**, *50*, 63534–63539. [[CrossRef](#)]



28. Grumezescu, A.M.; Gestal, M.C.; Holban, A.M.; Grumezescu, V.; Vasile, B.S.; Mogoanta, L.; Iordache, F.; Bleotu, C.; Mogosanu, G.D. Biocompatible Fe<sub>3</sub>O<sub>4</sub> increases the efficacy of amoxicillin delivery against Gram-positive and Gram-negative bacteria. *Molecules* **2014**, *19*, 5013–5027. [[CrossRef](#)] [[PubMed](#)]
29. Jiang, W.; Lai, K.L.; Hu, H.; Zeng, X.-B.; Lan, F.; Liu, F.; Liu, K.-X.; Wu, Y.; Gu, Z.-W. The effect of [Fe<sup>3+</sup>]/[Fe<sup>2+</sup>] molar ratio and iron salts concentration on the properties of superparamagnetic iron oxide nanoparticles in the water/ethanol/toluene system. *J. Nanoparticle Res.* **2011**, *13*, 5135–5145. [[CrossRef](#)]
30. Ali, A.; Zafar, H.; Zia, M.; Ul Haq, I.; Phull, A.R.; Ali, J.S.; Hussain, A. Synthesis, characterization, applications, and challenges of iron oxide nanoparticles. *Nanotechnol. Sci. Appl.* **2016**, *9*, 49–67. [[CrossRef](#)]
31. Shi, L.; Huang, J.; He, Y. Recyclable purification-evaporation systems based on Fe<sub>3</sub>O<sub>4</sub>@TiO<sub>2</sub> nanoparticles. *Energy Procedia* **2017**, *142*, 356–361. [[CrossRef](#)]
32. Anghel, A.G.; Grumezescu, A.M.; Chirea, M.; Grumezescu, V.; Socol, G.; Iordache, F.; Oprea, A.E.; Anghel, I.; Holban, A.M. MAPLE Fabricated Fe<sub>3</sub>O<sub>4</sub>@Cinnamomum verum Antimicrobial Surfaces for Improved Gastrostomy Tubes. *Molecules* **2014**, *19*, 8981–8994. [[CrossRef](#)]
33. Shen, L.; Qiao, Y.; Guo, Y.; Meng, S.; Yang, G.; Wu, M.; Zhao, J. Facile co-precipitation synthesis of shape-controlled magnetite nanoparticles. *Ceram. Int.* **2014**, *40*, 1519–1524. [[CrossRef](#)]
34. Singh, A.K.; Srivastava, O.N.; Singh, K. Shape and Size-Dependent Magnetic Properties of Fe<sub>3</sub>O<sub>4</sub> Nanoparticles Synthesized Using Piperidine. *Nanoscale Res. Lett.* **2017**, *12*, 298–305. [[CrossRef](#)]
35. Shah, S.T.; Yehya, W.A.; Saad, O.; Simarani, K.; Chowdhury, Z.; Alhadi, A.A.; Al-Ani, L.A. Surface Functionalization of Iron Oxide Nanoparticles with Gallic Acid as Potential Antioxidant and Antimicrobial Agents. *Nanomaterials* **2017**, *7*, 306. [[CrossRef](#)]
36. Zhu, N.; Ji, H.; Yu, P.; Niu, J.; Farooq, M.U.; Akram, M.W.; Udego, I.O.; Li, H.; Niu, X. Surface Modification of Magnetic Iron Oxide Nanoparticles. *Nanomaterials* **2018**, *8*, 810. [[CrossRef](#)] [[PubMed](#)]
37. Lassoued, A.; Dkhil, B.; Gadri, A.; Ammar, S. Control of the shape and size of iron oxide ( $\alpha$ -Fe<sub>2</sub>O<sub>3</sub>) nanoparticles synthesized through the chemical precipitation method. *Res. Phys.* **2017**, *7*, 3007–3015. [[CrossRef](#)]
38. Li, J.L.; Li, D.C.; Zhang, S.L.; Cui, H.C.; Wang, C. Analysis of the factors affecting the magnetic characteristics of nano-Fe<sub>3</sub>O<sub>4</sub> particles. *Chin. Sci. Bull.* **2011**, *8*, 803–810. [[CrossRef](#)]
39. Barbosa Salviano, L.; da Silva Cardoso, T.M.; Cordeiro Silva, G.; Silva Dantas, S.; de Mello Ferreira, A. Microstructural Assessment of Magnetite Nanoparticles (Fe<sub>3</sub>O<sub>4</sub>) Obtained by Chemical Precipitation Under Different Synthesis Conditions. *Mater. Res.* **2018**, *21*, e20170764. [[CrossRef](#)]
40. Meng, H.; Zhang, Z.; Zhao, F.; Qiu, T.; Yang, J. Orthogonal optimization design for preparation of Fe<sub>3</sub>O<sub>4</sub> nanoparticles via chemical coprecipitation. *Appl. Surf. Sci.* **2013**, *280*, 679–685. [[CrossRef](#)]
41. Andrade, A.I.; Souza, D.M.; Pereira, M.C.; Fabris, J.D.; Domingues, R.Z. pH effect on the synthesis of magnetite nanoparticles by the chemical reduction-precipitation method. *Quim. Nova* **2010**, *33*, 524–527. [[CrossRef](#)]
42. Ramadan, W.; Karim, M.; Hannoyer, B.; Saha, S. Effect of pH on the Structural and Magnetic Properties of Magnetite Nanoparticles Synthesized by Co-Precipitation. *Adv. Mater. Res.* **2012**, *324*, 129–132. [[CrossRef](#)]
43. Kalska-Szostko, B.; Wykowska, U.; Satula, D.; Nordblad, P. Thermal treatment of magnetite nanoparticles. *Beilstein J. Nanotechnol.* **2015**, *6*, 1385–1396. [[CrossRef](#)]
44. Niu, J.M.; Zheng, Z.G. Effect of Temperature on Fe<sub>3</sub>O<sub>4</sub> Nanoparticles prepared by Coprecipitation Method. *Adv. Mater. Res.* **2014**, *900*, 172–176. [[CrossRef](#)]
45. Saragi, T.; Depi, B.L.; Butarbutar, S.; Permana, B. The impact of synthesis temperature on magnetite nanoparticles size synthesized by co-precipitation method. *J. Phys. Conf. Ser.* **2018**, *1013*, 012190. [[CrossRef](#)]
46. Fayas, A.P.A.; Vinod, E.M.; Joseph, J.; Ganesan, R.; Pandey, R.K. Dependence of pH and surfactant effect in the synthesis of magneite (Fe<sub>3</sub>O<sub>4</sub>) nanoparticles and its properties. *J. Magn. Magn. Mater.* **2010**, *322*, 400–404. [[CrossRef](#)]
47. Filippousi, M.; Angelakeris, M.; Katsikini, M.; Paloura, E.; Esthimiopoulos, I.; Wang, Y.; Zamboulis, D.; Van Tendeloo, G. Surfactant Effects on the Structural and Magnetic Properties of Iron Oxide Nanoparticles. *J. Phys. Chem. C* **2014**, *118*, 16209–16217. [[CrossRef](#)]
48. Fatima, H.; Lee, D.-W.; Yun, H.J.; Kim, K.-S. Shape-controlled synthesis of magnetic Fe<sub>3</sub>O<sub>4</sub> nanoparticles with different iron precursors and capping agents. *RSC Adv.* **2018**, *8*, 22917–22923. [[CrossRef](#)]

49. Fotukian, S.M.; Barati, A.; Soleymani, M.; Alizadeh, A.M. Solvothermal synthesis of  $\text{CuFe}_2\text{O}_4$  and  $\text{Fe}_3\text{O}_4$  nanoparticles with high heating efficiency for magnetic hyperthermia application. *J. Alloys Compd.* **2019**, 152548–152556. [[CrossRef](#)]
50. Zhang, W.; Shen, F.; Hong, R. Solvothermal synthesis of magnetic  $\text{Fe}_3\text{O}_4$  microparticles via self-assembly of  $\text{Fe}_3\text{O}_4$  nanoparticles. *Particuology* **2011**, 9, 179–186. [[CrossRef](#)]
51. Qi, M.; Zhang, K.; Li, S.; Wu, J.; Pham-Hui, C.; Diao, X.; Xiao, D.; He, H. Superparamagnetic  $\text{Fe}_3\text{O}_4$  nanoparticles: Synthesis by a solvothermal process and functionalization for a magnetic targeted curcumin delivery system. *New J. Chem.* **2016**, 40, 4480–4491. [[CrossRef](#)]
52. Yan, J.; Mo, S.; Nie, J.; Chen, W.; Shen, X.; Hu, J.; Hao, G.; Tong, H. Hydrothermal synthesis of monodisperse  $\text{Fe}_3\text{O}_4$  nanoparticles based on modulation of tartaric acid. *Colloids Surf. A Physicochem. Eng. Asp.* **2009**, 340, 109–114. [[CrossRef](#)]
53. Lu, T.; Wang, J.; Yin, J.; Wang, A.; Wang, X.; Zhang, T. Surfactant effects on the microstructures of  $\text{Fe}_3\text{O}_4$  nanoparticles synthesized by microemulsion method. *Colloids Surf. A Physicochem. Eng. Asp.* **2013**, 436, 675–683. [[CrossRef](#)]
54. Su, H.; Han, X.; He, L.; Deng, L.; Yu, K.; Jiang, H.; Wu, C.; Jia, Q.; Shan, S. Synthesis and characterization of magnetic dextran nanogel doped with iron oxide nanoparticles as magnetic resonance imaging probe. *Int. J. Biol. Macromol.* **2019**, 128, 768–774. [[CrossRef](#)]
55. Pham, X.N.; Nguyen, T.P.; Pham, T.N.; Tran, N.T.T.; Tran, T.V.T. Synthesis and characterization of chitosan-coated magnetite nanoparticles and their application in curcumin drug delivery. *Adv. Nat. Sci. Nanosci. Nanotechnol.* **2016**, 7, 045010–045019. [[CrossRef](#)]
56. Unni, M.; Uhl, A.M.; Savliwala, S.; Savitzky, B.H.; Dhavalikar, R.; Garraud, N.; Arnold, D.P.; Kourkoutis, L.F.; Andrew, J.S.; Rinaldi, C. Thermal Decomposition Synthesis of Iron Oxide Nanoparticles with Diminished Magnetic Dead Layer by Controlled Addition of Oxygen. *ACS Nano* **2017**, 11, 2284–2303. [[CrossRef](#)] [[PubMed](#)]
57. Kumfer, B.M.; Shinoda, K.; Jeyadevan, B.; Kennedy, I.M. Gas-phase flame synthesis and properties of magnetic iron oxide nanoparticles with reduced oxidation state. *J. Aerosol Sci.* **2010**, 41, 257–265. [[CrossRef](#)] [[PubMed](#)]
58. Lassenberger, A.; Gruenewald, T.A.; van Oostrum, P.D.J.; Rennhofer, H.; Amenitsch, H.; Zirbs, R.; Lichtenegger, H.C.; Reimhult, E. Monodisperse Iron Oxide Nanoparticles by Thermal Decomposition: Elucidating Particle Formation by Second-Resolved in Situ Small-Angle X-ray Scattering. *Chem. Mater.* **2017**, 29, 4511–4522. [[CrossRef](#)] [[PubMed](#)]
59. Wei, Y.; Han, B.; Hu, X.; Lin, Y.; Wang, X.; Deng, X. Synthesis of  $\text{Fe}_3\text{O}_4$  Nanoparticles and their Magnetic Properties. *Procedia Eng.* **2012**, 27, 632–637. [[CrossRef](#)]
60. Xu, C.; Lu, X.; Dai, H. The Synthesis of Size-Adjustable Superparamagnetism  $\text{Fe}_3\text{O}_4$  Hollow Microspheres. *Nanoscale Res. Lett.* **2017**, 12, 234–244. [[CrossRef](#)] [[PubMed](#)]
61. Zhang, S.; Li, J.; Lykotrafitis, G.; Bao, G.; Suresh, S. Size-Dependent Endocytosis of Nanoparticles. *Adv. Mater.* **2009**, 21, 419–424. [[CrossRef](#)]
62. Bannunah, A.M.; Vllasaliu, D.; Lord, J.; Stolnik, S. Mechanisms of Nanoparticle Internalization and Transport Across an Intestinal Epithelial Cell Model: Effect of Size and Surface Charge. *Mol. Pharm.* **2014**, 11, 4363–4373. [[CrossRef](#)]
63. Shang, L.; Nienhaus, K.; Nienhaus, G.U. Engineered nanoparticles interacting with cells: Size matters. *J. Nanobiotechnol.* **2014**, 12, 5–16. [[CrossRef](#)]
64. Gratton, S.E.A.; Ropp, P.A.; Pohlhaus, P.D.; Luft, J.C.; Madden, V.J.; Napier, M.E.; DeSimone, J.M. The effect of particle design on cellular internalization pathways. *Proc. Natl. Acad. Sci. USA* **2008**, 105, 11613–11618. [[CrossRef](#)]
65. Xie, X.; Liao, J.; Shao, X.; Li, Q.; Lin, Y. The Effect of shape on Cellular Uptake of Gold Nanoparticles in the forms of Stars, Rods, and Triangles. *Sci. Rep.* **2017**, 7, 3827–3836. [[CrossRef](#)] [[PubMed](#)]
66. Toy, R.; Peiris, P.M.; Ghaghada, K.B.; Karathanasis, E. Shaping cancer nanomedicine: The effect of particle shape on the in vivo journey of nanoparticles. *Nanomedicine* **2014**, 9, 121–134. [[CrossRef](#)] [[PubMed](#)]
67. Chen, L.; Xiao, S.; Zhu, H.; Liang, H. Shape-dependent internalization kinetics of nanoparticles by membranes. *Soft Matter* **2016**, 12, 2632–2641. [[CrossRef](#)] [[PubMed](#)]

68. Cui, Y.N.; Xu, Q.X.; Davoodi, P.; Wang, D.P.; Wang, C.H. Enhanced intracellular delivery and controlled drug release of magnetic PLGA nanoparticles modified with transferrin. *Acta Pharmacol. Sin.* **2017**, *38*, 943–953. [[CrossRef](#)] [[PubMed](#)]
69. Georgieva, J.V.; Kalicharan, D.; Couraud, P.-O.; Romero, I.A.; Weksler, B.; Hoekstra, D.; Zuhorn, I.S. Surface Characteristics of Nanoparticles Determine Their Intracellular Fate in and Processing by Human Blood–Brain Barrier Endothelial Cells In Vitro. *Mol. Ther.* **2011**, *19*, 318–325. [[CrossRef](#)] [[PubMed](#)]
70. Arias, L.S.; Pessan, J.P.; Vieira, A.P.M.; Lima, T.M.T.; Delbem, A.C.B.; Monteiro, D.R. Iron Oxide Nanoparticles for Biomedical Applications: A Perspective on Synthesis, Drugs, Antimicrobial Activity, and Toxicity. *Antibiotics* **2018**, *7*, 46. [[CrossRef](#)]
71. Ma, P.; Luo, Q.; Chen, J.; Gan, Y.; Du, J.; Ding, S.; Xi, Z.; Yang, X. Intraperitoneal injection of magnetic Fe<sub>3</sub>O<sub>4</sub>-nanoparticle induces hepatic and renal tissue injury via oxidative stress in mice. *Int. J. Nanomed.* **2012**, *7*, 4809–4818. [[CrossRef](#)]
72. Wang, Y.; Qin, N.; Chen, S.; Zhao, J.; Yang, X. Oxidative-damage effect of Fe<sub>3</sub>O<sub>4</sub> nanoparticles on mouse hepatic and brain cells in vivo. *Front. Biol.* **2013**, *8*, 549–555. [[CrossRef](#)]
73. Wang, J.; Chen, Y.; Chen, B.; Ding, J.; Xia, G.; Gao, C.; Cheng, J.; Jin, N.; Zhou, Y.; Li, X.; et al. Pharmacokinetic parameters and tissue distribution of magnetic Fe<sub>3</sub>O<sub>4</sub> nanoparticles in mice. *Int. J. Nanomed.* **2010**, *5*, 861–866. [[CrossRef](#)]
74. Mejías, R.; Gutiérrez, L.; Salas, G.; Pérez-Yagüe, S.; Zotes, T.M.; Lázaro, F.J.; Morales, M.P.; Barber, D.F. Long term biotransformation and toxicity of dimercaptosuccinic acid-coated magnetic nanoparticles support their use in biomedical applications. *J. Control. Release* **2013**, *171*, 225–233. [[CrossRef](#)]
75. De Tercero, M.D.; Bruns, M.; Martínez, I.G.; Türk, M.; Fehrenbacher, U.; Jennewein, S.; Barner, L. Continuous Hydrothermal Synthesis of In Situ Functionalized Iron Oxide Nanoparticles: A General Strategy to Produce Metal Oxide Nanoparticles With Clickable Anchors. *Part. Part. Syst. Charact.* **2013**, *30*, 229–234. [[CrossRef](#)]
76. De Tercero, M.D.; González Martínez, I.; Herrmann, M.; Bruns, M.; Kübel, C.; Jennewein, S.; Fehrenbacher, U.; Barner, L.; Türk, M. Synthesis of in situ functionalized iron oxide nanoparticles presenting alkyne groups via a continuous process using near-critical and supercritical water. *J. Supercrit. Fluids* **2013**, *82*, 83–95. [[CrossRef](#)]
77. Karimzadeh, I.; Aghazadeh, M.; Doroudi, T.; Ganjali, M.R.; Kolivand, P.H. Superparamagnetic Iron Oxide (Fe<sub>3</sub>O<sub>4</sub>) Nanoparticles Coated with PEG/PEI for Biomedical Applications: A Facile and Scalable Preparation Route Based on the Cathodic Electrochemical Deposition Method. *Adv. Phys. Chem.* **2017**, *2017*, 9437487–9437494. [[CrossRef](#)]
78. Bini, R.A.; Marques, R.F.C.; Santos, F.J.; Chaker, J.A.; Jafellicci, M. Synthesis and functionalization of magnetite nanoparticles with different amino-functional alkoxysilanes. *J. Magn. Magn. Mater.* **2012**, *324*, 534–539. [[CrossRef](#)]
79. Rudakovskaya, P.G.; Gerasimov, V.M.; Metelkina, O.N.; Beloglazkina, E.K.; Savchenko, A.G.; Shchetinin, I.V.; Salikhov, S.V.; Abakumov, M.A.; Klyachko, N.L.; Golovin, Y.I.; et al. Synthesis and characterization of PEG-silane functionalized iron oxide(II, III) nanoparticles for biomedical application. *Nanotechnol. Russ.* **2015**, *10*, 896–903. [[CrossRef](#)]
80. Wang, L.; Li, Y.R.; Li, J.; Zou, S.; Stach, E.A.; Takeuchi, K.J.; Takeuchi, E.S.; Marschilok, A.C.; Wong, S.S. Correlating Preparative Approaches with Electrochemical Performance of Fe<sub>3</sub>O<sub>4</sub>-MWNT Composites Used as Anodes in Li-Ion Batteries. *J. Solid State Sci. Technol.* **2017**, *6*, M3122–M3131. [[CrossRef](#)]
81. Jokerst, J.V.; Lobovkina, T.; Zare, R.N.; Gambhir, S.S. Nanoparticle PEGylation for imaging and therapy. *Nanomedicine* **2011**, *6*, 715–728. [[CrossRef](#)]
82. Wei, W.; Bai, F.; Fan, H. Surfactant-Assisted Cooperative Self-Assembly of Nanoparticles into Active Nanostructures. *iScience* **2019**, *11*, 272–293. [[CrossRef](#)]
83. Chen, L.; Wu, L.; Liu, F.; Qi, X.; Ge, Y.; Shen, S. Azo-functionalized Fe<sub>3</sub>O<sub>4</sub> nanoparticles: A near-infrared light triggered drug delivery system for combined therapy of cancer with low toxicity. *J. Mater. Chem. B* **2016**, *4*, 3660–3669. [[CrossRef](#)]
84. Gawali, S.L.; Barick, K.C.; Shetake, N.G.; Rajan, V.; Pandey, B.N.; Kumar, N.N.; Priyadarsini, N.K.I.; Hassan, P.A. pH-Labile Magnetic Nanocarriers for Intracellular Drug Delivery to Tumor Cells. *ACS Omega* **2019**, *47*, 11728–11736. [[CrossRef](#)]

85. Sharma, K.S.; Ningthoujam, R.S.; Dubey, A.K.; Chattopadhyay, A.; Phapale, S.; Juluri, R.R.; Mukherjee, S.; Tewari, R.; Shetake, N.G.; Pandey, B.N.; et al. Synthesis and characterization of monodispersed water dispersible Fe<sub>3</sub>O<sub>4</sub> nanoparticles and in vitro studies on human breast carcinoma cell line under hyperthermia condition. *Sci. Rep.* **2018**, *8*, 14766–14777. [[CrossRef](#)] [[PubMed](#)]
86. Demin, A.M.; Krasnov, V.P.; Charushin, V.N. Covalent Surface Modification of Fe<sub>3</sub>O<sub>4</sub> Magnetic Nanoparticles with Alkoxy Silanes and Amino Acids. *Mendeleev Commun.* **2013**, *23*, 14–16. [[CrossRef](#)]
87. Arsalani, N.; Fattahi, H.; Nazarpour, M. Synthesis and characterization of PVP-functionalized superparamagnetic Fe<sub>3</sub>O<sub>4</sub> nanoparticles as an MRI contrast agent. *eXPRESS Polym. Lett.* **2010**, *4*, 329–338. [[CrossRef](#)]
88. Han, C.W.; Choksi, T.; Milligan, C.A.; Majumdar, P.; Manto, M.J.; Cui, Y.; Sang, X.; Unocic, R.R.; Zemlyanov, D.Y.; Wang, C.; et al. A Discovery of Strong Metal-Support Bonding in Nano-engineered Au-Fe<sub>3</sub>O<sub>4</sub> Dumbbell-like Nanoparticles by In-situ Transmission Electron Microscopy. *Nano Lett.* **2017**, *17*, 4576–4582. [[CrossRef](#)] [[PubMed](#)]
89. Abbas, M.; Torati, S.R.; Iqbal, S.A.; Kim, C.G. A novel and rapid approach for the synthesis of biocompatible and highly stable Fe<sub>3</sub>O<sub>4</sub>/SiO<sub>2</sub> and Fe<sub>3</sub>O<sub>4</sub>/C core/shell nanocubes and nanorods. *New J. Chem.* **2017**, *41*, 2724–2734. [[CrossRef](#)]
90. Khosroshahi, M.E.; Ghazanfari, L.; Tahriri, M. Characterisation of binary (Fe<sub>3</sub>O<sub>4</sub>/SiO<sub>2</sub>) biocompatible nanocomposites as magnetic fluid. *J. Exp. Nanosci.* **2011**, *6*, 580–595. [[CrossRef](#)]
91. Guo, X.; Mao, F.; Wang, W.; Yang, Y.; Bai, Z. Sulfhydryl-Modified Fe<sub>3</sub>O<sub>4</sub>@SiO<sub>2</sub> Core/Shell Nanocomposite: Synthesis and Toxicity Assessment in Vitro. *ACS Appl. Mater. Interfaces* **2015**, *7*, 14983–14991. [[CrossRef](#)]
92. Nikmah, A.; Taufiq, A.; Hidayat, A. Synthesis and Characterization of Fe<sub>3</sub>O<sub>4</sub>/SiO<sub>2</sub> nanocomposites. *IOP Conf. Ser. Earth Environ. Sci.* **2019**, *276*, 012046.
93. Ding, H.L.; Zhang, X.Y.; Wang, S.; Xu, J.M.; Xu, S.C.; Li, G.H. Fe<sub>3</sub>O<sub>4</sub>@SiO<sub>2</sub> Core/Shell Nanoparticles: The Silica Coating Regulations with a Single Core for Different Core Sizes and Shell Thicknesses. *Chem. Mater.* **2012**, *24*, 4572–4580. [[CrossRef](#)]
94. Liu, C.Y.; Puig, T.; Obradors, X.; Ricart, S.; Ros, J. Ultra-fast microwave-assisted reverse microemulsion synthesis of Fe<sub>3</sub>O<sub>4</sub>@SiO<sub>2</sub> core-shell nanoparticles as a highly recyclable silver nanoparticle catalytic platform in the reduction of 4-nitroaniline. *RSC Adv.* **2016**, *6*, 88762–88769. [[CrossRef](#)]
95. Zhang, Y.; Yan, J.; Liu, S. Biocompatibility and biomedical applications of functionalized mesoporous silica nanoparticles. *Biointerface Res. Appl. Chem.* **2014**, *4*, 767–775.
96. Tang, F.; Li, L.; Chen, D. Mesoporous Silica Nanoparticles: Synthesis, Biocompatibility and Drug Delivery. *Adv. Mater.* **2012**, *24*, 1504–1534. [[CrossRef](#)]
97. Asefa, T.; Tao, Z. Biocompatibility of Mesoporous Silica Nanoparticles. *Chem. Res. Toxicol.* **2012**, *25*, 2265–2284. [[CrossRef](#)]
98. Narayan, R.; Nayak, U.Y.; Raichur, A.M.; Garg, S. Mesoporous Silica Nanoparticles: A Comprehensive Review on Synthesis and Recent Advances. *Pharmaceutics* **2018**, *10*, 118. [[CrossRef](#)] [[PubMed](#)]
99. Isa, E.D.M.; Ahmad, H.; Rahman, M.B.A. Optimization of Synthesis Parameters of Mesoporous Silica Nanoparticles Based on Ionic Liquid by Experimental Design and Its Application as a Drug Delivery Agent. *J. Nanomater.* **2019**, *2019*, 4982054–4982062. [[CrossRef](#)]
100. Jorge, J.; Verelst, M.; de Castro, G.R.; Martines, M.A.U. Synthesis parameters for control of mesoporous silica nanoparticles (MSNs). *Biointerface Res. Appl. Chem.* **2016**, *6*, 1520–1524.
101. Sun, J.-G.; Jiang, Q.; Zhang, X.-P.; Shan, K.; Liu, B.-H.; Zhao, C.; Yan, B. Mesoporous silica nanoparticles as a delivery system for improving antiangiogenic therapy. *Int. J. Nanomed.* **2019**, *14*, 1489–1501. [[CrossRef](#)] [[PubMed](#)]
102. Vallet-Regí, M.; Colilla, M.; Izquierdo-Barba, I.; Manzano, M. Mesoporous Silica Nanoparticles for Drug Delivery: Current Insights. *Molecules* **2017**, *23*, 47. [[CrossRef](#)] [[PubMed](#)]
103. Ye, F.; Laurent, S.; Fornara, A.; Astolfi, L.; Qin, J.; Roch, A.; Martini, A.; Toprak, M.S.; Muller, R.N.; Muhammed, M. Uniform mesoporous silica coated iron oxide nanoparticles as a highly efficient, nontoxic MRI T2 contrast agent with tunable proton relaxivities. *Contrast Media Mol. Imaging* **2012**, *7*, 460–468. [[CrossRef](#)] [[PubMed](#)]
104. Sharafi, Z.; Bakhshi, B.; Javidi, J.; Adrangi, S. Synthesis of Silica-coated Iron Oxide Nanoparticles: Preventing Aggregation without Using Additives or Seed Pretreatment. *Iran. J. Pharm. Res.* **2018**, *17*, 386–395. [[PubMed](#)]
105. Yin, N.Q.; Wu, P.; Yang, T.H.; Wang, M. Preparation and study of a mesoporous silica-coated Fe<sub>3</sub>O<sub>4</sub> photothermal nanoprobe. *RSC Adv.* **2017**, *7*, 9123–9129. [[CrossRef](#)]



106. Venkatathri, N. Synthesis of mesoporous silica nanosphere using different templates. *Solid State Commun.* **2007**, *143*, 493–497. [[CrossRef](#)]
107. Kipkemboi, P.; Fogden, A.; Alfredsson, V.; Flostroem, K. Triblock Copolymers as Templates in Mesoporous Silica Formation: Structural Dependence on Polymer Chain Length and Synthesis Temperature. *Langmuir* **2001**, *17*, 5398–5402. [[CrossRef](#)]
108. Peralta, M.E.; Jadhav, S.A.; Magnacca, G.; Scalarone, D.; Mártire, D.O.; Parolo, M.E.; Carlos, L. Synthesis and in vitro testing of thermoresponsive polymer-grafted core-shell magnetic mesoporous silica nanoparticles for efficient controlled and targeted drug delivery. *J. Colloid Interface Sci.* **2019**, *544*, 198–205. [[CrossRef](#)]
109. Park, S.S.; Jung, M.H.; Lee, Y.-S.; Bae, J.-H.; Kim, S.-H.; Ha, C.-S. Functionalised mesoporous silica nanoparticles with excellent cytotoxicity against various cancer cells for pH-responsive and controlled drug delivery. *Mater. Des.* **2019**, *184*, 108187–108197. [[CrossRef](#)]
110. Li, T.; Geng, T.; Md, A.; Banerjee, P.; Wang, B. Novel scheme for rapid synthesis of hollow mesoporous silica nanoparticles (HMSNs) and their application as an efficient delivery carrier for oral bioavailability improvement of poorly water-soluble BCS type II drugs. *Colloids Surf. B Biointerfaces* **2019**, *176*, 185–193. [[CrossRef](#)] [[PubMed](#)]
111. Rowley, J.; Abu-Zahra, N.H. Synthesis and characterization of polyethersulfone membranes impregnated with (3-aminopropyltriethoxysilane) APTES-Fe<sub>3</sub>O<sub>4</sub> nanoparticles for As(V) removal from water. *J. Environ. Chem. Eng.* **2019**, *7*, 102875–102885. [[CrossRef](#)]
112. Liang, X.X.; Ouyang, X.K.; Wang, S.; Yang, L.-Y.; Huang, F.; Ji, C.; Chen, X. Efficient adsorption of Pb(II) from aqueous solutions using aminopropyltriethoxysilane-modified magnetic attapulgite@chitosan (APTS-Fe<sub>3</sub>O<sub>4</sub>/APT@CS) composite hydrogel beads. *Int. J. Biol. Macromol.* **2019**, *137*, 741–750. [[CrossRef](#)]
113. Langeroudi, M.P.; Binaeian, E. Tannin-APTES modified Fe<sub>3</sub>O<sub>4</sub> nanoparticles as a carrier of Methotrexate drug: Kinetic, isotherm and thermodynamic studies. *Mater. Chem. Phys.* **2018**, *218*, 210–217. [[CrossRef](#)]
114. Arum, Y.; Yun-Ok, O.; Kang, H.W.; Seok-Hwan, A.; Junghwan, O. Chitosan-Coated Fe<sub>3</sub>O<sub>4</sub> Magnetic Nanoparticles as Carrier of Cisplatin for Drug Delivery. *Fish. Aquat. Sci.* **2015**, *18*, 89–98. [[CrossRef](#)]
115. Zhang, S.; Zhang, Y.; Liu, J.; Xu, Q.; Xiao, H.; Wang, X.; Xu, H.; Zhou, J. Thiol modified Fe<sub>3</sub>O<sub>4</sub>@SiO<sub>2</sub> as a robust, high effective, and recycling magnetic sorbent for mercury removal. *Chem. Eng. J.* **2013**, *226*, 30–38. [[CrossRef](#)]
116. Badragheh, S.; Zeeb, M.; Olyai, M.R.T.B. Silica-coated magnetic iron oxide functionalized with hydrophobic polymeric ionic liquid: a promising nanoscale sorbent for simultaneous extraction of antidiabetic drugs from human plasma prior to their quantitation by HPLC. *RSC Adv.* **2018**, *8*, 30550–30561. [[CrossRef](#)]
117. Rego, G.N.A.; Mamani, J.B.; Souza, T.K.F.; Nucci, M.P.; Silva, H.R.D.; Gamarra, L.F. Therapeutic evaluation of magnetic hyperthermia using Fe<sub>3</sub>O<sub>4</sub>-aminosilane-coated iron oxide nanoparticles in glioblastoma animal model. *Einstein* **2019**, *17*, 1–9. [[CrossRef](#)] [[PubMed](#)]
118. Shaleri Kardar, Z.S.; Beyki, M.H.; Shemirani, F. Bifunctional aminosilane-functionalized Fe<sub>3</sub>O<sub>4</sub> nanoparticles as efficient sorbent for preconcentration of cobalt ions from food and water samples. *Res. Chem. Intermed.* **2017**, *43*, 4079–4096. [[CrossRef](#)]
119. Tian, F.; Chen, G.; Yi, P.; Zhang, J.; Li, A.; Zhang, J.; Zheng, L.; Deng, Z.; Shi, Q.; Peng, R.; et al. Fates of Fe<sub>3</sub>O<sub>4</sub> and Fe<sub>3</sub>O<sub>4</sub>@SiO<sub>2</sub> nanoparticles in human mesenchymal stem cells assessed by synchrotron radiation-based techniques. *Biomaterials* **2014**, *35*, 6412–6421. [[CrossRef](#)] [[PubMed](#)]
120. Mostafaei, M.; Hosseini, S.N.; Khatami, M.; Javidanbardan, A.; Sepahy, A.A.; Asadi, E. Isolation of recombinant Hepatitis B surface antigen with antibody-conjugated superparamagnetic Fe<sub>3</sub>O<sub>4</sub>/SiO<sub>2</sub> core-shell nanoparticles. *Protein Expr. Purif.* **2018**, *145*, 1–6. [[CrossRef](#)]
121. Fan, Q.; Guan, Y.; Zhang, Z.; Xu, G.; Yang, Y.; Guo, C. A new method of synthesis well-dispersion and dense Fe<sub>3</sub>O<sub>4</sub>@SiO<sub>2</sub> magnetic nanoparticles for DNA extraction. *Chem. Phys. Lett.* **2019**, *715*, 7–13. [[CrossRef](#)]
122. Gan, Q.; Lu, X.; Yuan, Y.; Qian, J.; Zhou, H.; Lu, X.; Shi, J.; Liu, C. A magnetic, reversible pH-responsive nanogated ensemble based on Fe<sub>3</sub>O<sub>4</sub> nanoparticles-capped mesoporous silica. *Biomaterials* **2011**, *32*, 1932–1942. [[CrossRef](#)]
123. Cui, J.; Sun, B.; Lin, T.; Feng, Y.; Jia, S. Enzyme shielding by mesoporous organosilica shell on Fe<sub>3</sub>O<sub>4</sub>@silica yolk-shell nanospheres. *Int. J. Biol. Macromol.* **2018**, *117*, 673–682. [[CrossRef](#)]
124. Asgari, M.; Soleymani, M.; Miri, T.; Barati, A. A robust method for fabrication of monodisperse magnetic mesoporous silica nanoparticles with core-shell structure as anticancer drug carriers. *J. Mol. Liquids* **2019**, *292*, 111367–111375. [[CrossRef](#)]



125. Wang, J.; Yang, J.; Li, X.; Wang, D.; Wei, B.; Song, H.; Li, X.; Fu, S. Preparation and photocatalytic properties of magnetically reusable Fe<sub>3</sub>O<sub>4</sub>@ZnO core/shell nanoparticles. *Phys. E* **2016**, *75*, 66–71. [[CrossRef](#)]
126. Zhang, L.; Wu, Z.; Chen, L.; Zhang, L.; Li, X.; Xu, H.; Wang, H.; Zhu, G. Preparation of magnetic Fe<sub>3</sub>O<sub>4</sub>/TiO<sub>2</sub>/Ag composite microspheres with enhanced photocatalytic activity. *Solid State Sci.* **2016**, *52*, 42–48. [[CrossRef](#)]
127. Choi, K.H.; Min, J.; Park, S.Y.; Park, B.J.; Jung, J.S. Enhanced photocatalytic degradation of tri-chlorophenol by Fe<sub>3</sub>O<sub>4</sub>@TiO<sub>2</sub>@Au photocatalyst under visible-light. *Ceram. Int.* **2019**, *45*, 9477–9482. [[CrossRef](#)]
128. Li, Y.; Liu, J.; Zhong, Y.; Zhang, J.; Wang, Z.; Wang, L.; An, Y.; Lin, M.; Gao, Z.; Zhang, D. Biocompatibility of Fe<sub>3</sub>O<sub>4</sub>@Au composite magnetic nanoparticles in vitro and in vivo. *Int. J. Nanomed.* **2011**, *6*, 2805–2819. [[CrossRef](#)]
129. Nalluri, S.R.; Nagarjuna, R.; Patra, D.; Ganesan, R.; Balaji, G. Large Scale Solid-state Synthesis of Catalytically Active Fe<sub>3</sub>O<sub>4</sub>@M (M = Au, Ag and Au-Ag alloy) Core-shell Nanostructures. *Sci. Rep.* **2019**, *9*, 6603–6614. [[CrossRef](#)] [[PubMed](#)]
130. Ma, L.L.; Borwankar, A.U.; Willsey, B.W.; Yoon, K.Y.; Tam, J.O.; Sokolov, K.V.; Feldman, M.D.; Milner, T.E.; Johnston, K.P. Growth of textured thin Au coatings on iron oxide nanoparticles with near infrared absorbance. *Nanotechnology* **2013**, *24*, 025606–025620. [[CrossRef](#)] [[PubMed](#)]
131. Sanchez, L.M.; Alvarez, V.A. Advances in Magnetic Noble Metal/Iron-Based Oxide Hybrid Nanoparticles as Biomedical Devices. *Bioengineering* **2019**, *6*, 75. [[CrossRef](#)] [[PubMed](#)]
132. Ma, C.; Shao, H.; Zhan, S.; Hou, P.; Zhang, X.; Chai, Y.; Liu, H. Bi-phase dispersible Fe<sub>3</sub>O<sub>4</sub>@Au core-shell multifunctional nanoparticles: Synthesis, characterization and properties. *Compos. Interfaces* **2019**, *26*, 537–549. [[CrossRef](#)]
133. Zhu, H.; Zhu, E.; Ou, G.; Gao, L.; Chen, J. Fe<sub>3</sub>O<sub>4</sub>-Au and Fe<sub>2</sub>O<sub>3</sub>-Au Hybrid Nanorods: Layer-by-Layer Assembly Synthesis and Their Magnetic and Optical Properties. *Nanoscale Res. Lett.* **2010**, *5*, 1755–1761. [[CrossRef](#)] [[PubMed](#)]
134. Lu, Q.; Dai, X.; Zhang, P.; Tan, X.; Zhong, Y.; Yao, C.; Song, M.; Song, G.; Zhang, G.; Peng, G.; et al. Fe<sub>3</sub>O<sub>4</sub>@Au composite magnetic nanoparticles modified with cetuximab for targeted magneto-photothermal therapy of glioma cells. *Int. J. Nanomed.* **2018**, *13*, 2491–2505. [[CrossRef](#)] [[PubMed](#)]
135. Wang, L.; Wang, L.; Luo, J.; Fan, Q.; Suzuki, M.; Suzuki, I.S.; Engelhard, M.H.; Lin, Y.; Kim, N.; Jian, Q.; et al. Monodispersed Core-Shell Fe<sub>3</sub>O<sub>4</sub>@Au Nanoparticles. *J. Phys. Chem. B* **2005**, *109*, 21593–21601. [[CrossRef](#)] [[PubMed](#)]
136. Xu, Z.; Hou, Y.; Sun, S. Magnetic Core/Shell Fe<sub>3</sub>O<sub>4</sub>/Au and Fe<sub>3</sub>O<sub>4</sub>/Au/Ag Nanoparticles with Tunable Plasmonic Properties. *J. Am. Chem. Soc.* **2007**, *129*, 8698–8699. [[CrossRef](#)] [[PubMed](#)]
137. Hu, Y.; Wang, R.; Wang, S.; Ding, L.; Li, J.; Luo, Y.; Wang, X.; Shen, M.; Shi, X. Multifunctional Fe<sub>3</sub>O<sub>4</sub>@Au core/shell nanostars: A unique platform for multimode imaging and photothermal therapy of tumors. *Sci. Rep.* **2016**, *6*, 28325–28337. [[CrossRef](#)] [[PubMed](#)]
138. Ge, Y.; Zhong, Y.; Ji, G.; Lu, Q.; Dai, X.; Guo, Z.; Zhang, P.; Peng, G.; Zhang, K.; Li, Y. Preparation and characterization of Fe<sub>3</sub>O<sub>4</sub>@Au-C225 composite targeted nanoparticles for MRI of human glioma. *PLoS ONE* **2018**, *13*, e0195703. [[CrossRef](#)]
139. Kang, N.; Xu, D.; Han, Y.; Lv, X.; Chen, Z.; Zhou, T.; Ren, L.; Zhou, X. Magnetic targeting core/shell Fe<sub>3</sub>O<sub>4</sub>/Au nanoparticles for magnetic resonance/photoacoustic dual-modal imaging. *Mater. Sci. Eng. C* **2019**, *98*, 545–549. [[CrossRef](#)]
140. Klein, S.; Hübner, J.; Menter, C.; Distel, L.V.R.; Neuhuber, W.; Kryschi, C. A Facile One-Pot Synthesis of Water-Soluble, Patchy Fe<sub>3</sub>O<sub>4</sub>-Au Nanoparticles for Application in Radiation Therapy. *Appl. Sci.* **2019**, *9*, 15. [[CrossRef](#)]
141. Hu, R.; Zheng, M.; Wu, J.; Li, C.; Shen, D.; Yang, D.; Li, L.; Ge, M.; Chang, Z.; Dong, W. Core-Shell Magnetic Gold Nanoparticles for Magnetic Field-Enhanced Radio-Photothermal Therapy in Cervical Cancer. *Nanomaterials* **2017**, *7*, 111. [[CrossRef](#)]
142. Li, J.; Hu, Y.; Yang, J.; Wei, P.; Sun, W.; Shen, M.; Zhang, G.; Shi, X. Hyaluronic acid-modified Fe<sub>3</sub>O<sub>4</sub>@Au core/shell nanostars for multimodal imaging and photothermal therapy of tumors. *Biomaterials* **2015**, *38*, 10–21. [[CrossRef](#)]
143. Park, S.I.; Chung, S.H.; Kim, H.C.; Lee, S.G.; Lee, S.J.; Kim, H.; Kim, H.; Jeong, S.W. Prolonged heating of Fe<sub>3</sub>O<sub>4</sub>-Au hybrid nanoparticles in a radiofrequency solenoid coil. *Colloids Surf. A Physicochem. Eng. Asp.* **2018**, *538*, 304–309. [[CrossRef](#)]

144. Her, S.; Jaffray, D.A.; Allen, C. Gold nanoparticles for applications in cancer radiotherapy: Mechanisms and recent advancements. *Adv. Drug Deliv. Rev.* **2017**, *109*, 84–101. [[CrossRef](#)]
145. Yu, B.; Liu, T.; Du, X.; Luo, Z.; Zheng, W.; Chen, T. X-ray-responsive selenium nanoparticles for enhanced cancer chemo-radiotherapy. *Colloids Surf. B Biointerfaces* **2016**, *139*, 180–189. [[CrossRef](#)] [[PubMed](#)]
146. Mattea, F.; Vedelago, J.; Malano, F.; Gomez, C.; Strumia, M.C.; Valente, M. Silver nanoparticles in X-ray biomedical applications. *Radiat. Phys. Chem.* **2017**, *130*, 442–450. [[CrossRef](#)]
147. Berbeco, R.I.; Ngwa, W.; Makrigiorgos, G.M. Localized Dose Enhancement to Tumor Blood Vessel Endothelial Cells via Megavoltage X-rays and Targeted Gold Nanoparticles: New Potential for External Beam Radiotherapy. *Int. J. Radiat. Oncol. Biol. Phys.* **2011**, *81*, 270–276. [[CrossRef](#)] [[PubMed](#)]
148. Generalov, R.; Kuan, W.B.; Chen, W.; Kristensen, S.; Juzenas, P. Radiosensitizing effect of zinc oxide and silica nanocomposites on cancer cells. *Colloids Surf. B Biointerfaces* **2015**, *129*, 79–86. [[CrossRef](#)]
149. Wolfe, T.; Chatterjee, D.; Lee, J.; Grant, J.D.; Bhattarai, S.; Taylor, R.; Goodrich, G.; Nicolucci, P.; Krishnan, S. Targeted gold nanoparticles enhance radiosensitization of prostate tumors to megavoltage radiation therapy in vivo. *Nanomedicine* **2015**, *11*, 1277–1283. [[CrossRef](#)]
150. Miladi, I.; Aloy, M.T.; Armandy, E.; Mowat, P.; Kryza, D.; Magne, N.; Tillement, O.; Lux, F.; Billotey, C.; Janier, M.; et al. Combining ultrasmall gadolinium-based nanoparticles with photon irradiation overcomes radioresistance of head and neck squamous cell carcinoma. *Nanomedicine* **2015**, *11*, 247–257. [[CrossRef](#)]
151. Liu, Y.; Liu, X.; Jin, X.; He, P.; Zheng, X.; Dai, Z.; Ye, F.; Zhao, T.; Chen, W.; Li, Q. The dependence of radiation enhancement effect on the concentration of gold nanoparticles exposed to low- and high- LET radiations. *Eur. J. Med. Phys.* **2015**, *31*, 210–218. [[CrossRef](#)]
152. Roduner, E. Size matters: Why nanomaterials are different. *Chem. Soc. Rev.* **2006**, *35*, 583–592. [[CrossRef](#)]
153. Eustis, S.; El-Sayed, M.A. Why gold nanoparticles are more precious than pretty gold: Noble metal surface plasmon resonance and its enhancement of the radiative and nonradiative properties of nanocrystals of different shapes. *Chem. Soc. Rev.* **2006**, *35*, 209–217. [[CrossRef](#)]
154. Prado-Gotor, R.; Grueso, E. A kinetic study of the interaction of DNA with gold nanoparticles: Mechanistic aspects of the interaction. *Phys. Chem. Chem. Phys.* **2011**, *13*, 1479–1489. [[CrossRef](#)]
155. Li, K.; Zhao, X.; Hammer, B.K.; Du, S.; Chen, Y. Nanoparticles Inhibit DNA Replication by Binding to DNA: Modeling and Experimental Validation. *ACS Nano* **2013**, *7*, 9664–9674. [[CrossRef](#)] [[PubMed](#)]
156. Glazer, E.S.; Curley, S.A. Non-invasive radiofrequency ablation of malignancies mediated by quantum dots, gold nanoparticles and carbon nanotubes. *Ther. Deliv.* **2011**, *2*, 1325–1330. [[CrossRef](#)] [[PubMed](#)]
157. Li, J.; Liang, Z.; Zhong, X.; Zhao, Z.; Li, J. Study on the Thermal Characteristics of Fe<sub>3</sub>O<sub>4</sub> Nanoparticles and Gelatin Compound for Magnetic Fluid Hyperthermia in Radiofrequency Magnetic Field. *IEEE Trans. Magn.* **2014**, *50*, 1–4. [[CrossRef](#)]
158. Liu, B.; Zhou, J.; Zhang, B.; Qu, J. Synthesis of Ag@Fe<sub>3</sub>O<sub>4</sub> Nanoparticles for Photothermal Treatment of Ovarian Cancer. *J. Nanomater.* **2019**, *2019*, 6457968–6457976. [[CrossRef](#)]
159. Wang, J.; Sun, Y.; Wang, L.; Zhu, X.; Zhang, H.; Song, D. Surface plasmon resonance biosensor based on Fe<sub>3</sub>O<sub>4</sub>/Au nanocomposites. *Colloids Surf. B Biointerfaces* **2010**, *81*, 600–606. [[CrossRef](#)]
160. Zhao, Y.; Zhang, W.; Lin, Y.; Du, D. The vital function of Fe<sub>3</sub>O<sub>4</sub>@Au nanocomposite for hydrolase biosensor design and its application in detection of methyl parathion. *Nanoscale* **2013**, *5*, 1121–1126. [[CrossRef](#)]
161. Liu, F.M.; Nie, J.; Qin, Y.N.; Yin, W.; Hou, C.J.; Huo, D.Q.; He, B.; Xia, T.C. A biomimetic sensor based on specific receptor ETBD and Fe<sub>3</sub>O<sub>4</sub>@Au/MoS<sub>2</sub>/GN for signal enhancement shows highly selective electrochemical response to ultra-trace lead (II). *J. Solid State Electrochem.* **2017**, *21*, 3257–3268. [[CrossRef](#)]
162. Li, S.; Liang, J.; Zhou, Z.; Li, G. An electrochemical immunosensor for AFP measurement based on the magnetic Fe<sub>3</sub>O<sub>4</sub>@Au@CS nanomaterials. *IOP Conf. Ser. Mater. Sci. Eng.* **2018**, *382*, 022017. [[CrossRef](#)]
163. Cui, Y.R.; Hong, C.; Zhou, Y.L.; Li, Y.; Gao, X.M.; Zhang, X.X. Synthesis of orientedly bioconjugated core/shell Fe<sub>3</sub>O<sub>4</sub>@Au magnetic nanoparticles for cell separation. *Talanta* **2011**, *85*, 1246–1252. [[CrossRef](#)]
164. Li, J.; Zou, S.; Gao, J.; Liang, J.; Zhou, H.; Liang, L.; Wu, W. Block copolymer conjugated Au-coated Fe<sub>3</sub>O<sub>4</sub> nanoparticles as vectors for enhancing colloidal stability and cellular uptake. *J. Nanobiotechnol.* **2017**, *15*, 56–67. [[CrossRef](#)]
165. Li, Y.; Yun, K.H.; Lee, H.; Goh, S.H.; Suh, Y.G.; Choi, Y. Porous platinum nanoparticles as a high-Z and oxygen generating nanozyme for enhanced radiotherapy in vivo. *Biomaterials* **2019**, *197*, 12–19. [[CrossRef](#)] [[PubMed](#)]

166. Samadi, A.; Klingberg, H.; Jauffred, L.; Kjaer, A.; Bendix, P.M.; Oddershede, L.B. Platinum nanoparticles: A non-toxic, effective and thermally stable alternative plasmonic material for cancer therapy and bioengineering. *Nanoscale* **2018**, *10*, 9097–9107. [[CrossRef](#)] [[PubMed](#)]
167. Ma, M.; Xie, J.; Zhang, Y.; Chen, Z.; Gu, N. Fe<sub>3</sub>O<sub>4</sub>@Pt nanoparticles with enhanced peroxidase-like catalytic activity. *Mater. Lett.* **2013**, *105*, 36–39. [[CrossRef](#)]
168. Wu, D.; Ma, H.; Zhang, Y.; Jia, H.; Yan, T.; Wei, Q. Corallite-like Magnetic Fe<sub>3</sub>O<sub>4</sub>@MnO<sub>2</sub>@Pt Nanocomposited as Multiple Signal Amplifiers for the Detection of Carcinoembryonic Antigen. *ACS Appl. Mater. Interfaces* **2015**, *7*, 18786–18793. [[CrossRef](#)] [[PubMed](#)]
169. Khaghani, S.; Ghanbari, D.J. Magnetic and photo-catalyst Fe<sub>3</sub>O<sub>4</sub>-Ag nanocomposite: Green preparation of silver and magnetite nanoparticles by garlic extract. *Mater. Sci. Mater. Electron.* **2017**, *28*, 2877–2886. [[CrossRef](#)]
170. Gao, G.; Wang, K.; Huang, P.; Zhang, Y.; Bao, C.; Cui, D. Superparamagnetic Fe<sub>3</sub>O<sub>4</sub>-Ag hybrid nanocrystals as a potential contrast agent for CT imaging. *Cryst. Eng. Commun.* **2012**, *14*, 7556–7559. [[CrossRef](#)]
171. Sadat, M.E.; Baghbador, M.K.; Dunn, A.W.; Wagner, H.P.; Ewing, R.C.; Zhang, J.; Xu, H.; Pauletti, G.M.; Mast, D.B.; Shi, D. Photoluminescence and photothermal effect of Fe<sub>3</sub>O<sub>4</sub> nanoparticles for medical imaging and therapy. *Appl. Phys. Lett.* **2014**, *105*, 091903. [[CrossRef](#)]
172. Zhang, X.; Liu, Z.; Lou, Z.; Chen, F.; Chang, S.; Miao, Y.; Zhou, Z.; Hu, X.; Feng, J.; Ding, Q.; et al. Radiosensitivity enhancement of Fe<sub>3</sub>O<sub>4</sub>@Ag nanoparticles on human glioblastoma cells. *Artif. Cells Nanomed. Biotechnol.* **2018**, *46* (Suppl. S1), 975–984. [[CrossRef](#)]
173. Nguyen, T.N.L.; Do, T.V.; Nguyen, T.V.; Dao, P.H.; Trinh, V.T.; Mac, V.P.; Nguyen, A.H.; Dinh, D.A.; Nguyen, T.A.; Vo, T.K.A.; et al. Antimicrobial activity of acrylic polyurethane/Fe<sub>3</sub>O<sub>4</sub>-Ag nanocomposite coating. *Prog. Org. Coat.* **2019**, *132*, 15–20. [[CrossRef](#)]
174. Chang, M.; Lin, W.S.; Xiao, W.; Chen, Y.N. Antibacterial Effects of Magnetically-Controlled Ag/Fe<sub>3</sub>O<sub>4</sub> Nanoparticles. *Materials* **2018**, *11*, 659. [[CrossRef](#)]
175. Brollo, M.E.F.; Lopez-Ruiz, R.; Muraca, D.; Figueroa, S.J.A.; Pirola, K.R.; Knobel, M. Compact Ag@Fe<sub>3</sub>O<sub>4</sub> Core-shell Nanoparticles by Means of Single-step Thermal Decomposition Reaction. *Sci. Rep.* **2014**, *4*, 6839–6845. [[CrossRef](#)] [[PubMed](#)]
176. Kim, M.; Kim, J. Synergistic interaction between pseudocapacitive Fe<sub>3</sub>O<sub>4</sub> nanoparticles and highly porous silicon carbide for high-performance electrodes as electrochemical supercapacitors. *Nanotechnology* **2017**, *28*, 195401–195414.
177. Fan, H.; Niu, R.; Duan, J.; Liu, W.; Shen, W. Fe<sub>3</sub>O<sub>4</sub>@Carbon Nanosheets for All-Solid-State Supercapacitor Electrodes. *ACS Appl. Mater. Interfaces* **2016**, *8*, 19475–19483. [[CrossRef](#)] [[PubMed](#)]
178. Zeng, Z.; Zhao, H.; Wang, J.; Lv, P.; Zhang, T.; Xia, Q. Nanostructured Fe<sub>3</sub>O<sub>4</sub>@C as anode material for lithium-ion batteries. *J. Power Sources* **2014**, *248*, 15–21. [[CrossRef](#)]
179. Zhang, Z.; Kong, J. Novel magnetic Fe<sub>3</sub>O<sub>4</sub>@C nanoparticles as adsorbents for removal of organic dyes from aqueous solution. *J. Hazard. Mater.* **2011**, *193*, 325–329. [[CrossRef](#)] [[PubMed](#)]
180. Mao, G.Y.; Yang, W.J.; Bu, F.X.; Jiang, D.M.; Zhao, Z.J.; Zhang, Q.H.; Fang, Q.C.; Jiang, J.S. One-step hydrothermal synthesis of Fe<sub>3</sub>O<sub>4</sub>@C nanoparticles with great performance in biomedicine. *J. Mater. Chem. B* **2014**, *2*, 4481–4488. [[CrossRef](#)]
181. Da Costa, T.R.; Baldi, E.; Figueró, A.; Colpani, G.L.; Silva, L.L.; Zanetti, M.; de Mello, J.M.M.; Fiori, M.A. Fe<sub>3</sub>O<sub>4</sub>@C core-shell nanoparticles as adsorbent of ionic zinc: Evaluating of the adsorptive capacity. *Mater. Res.* **2019**, *22* (Suppl. S1), e20180847. [[CrossRef](#)]
182. Hein, C.D.; Liu, X.M.; Wang, D. Click chemistry, a powerful tool for pharmaceutical sciences. *Pharm. Res.* **2008**, *25*, 2216–2230. [[CrossRef](#)]
183. Campidelli, S. Click Chemistry for Carbon Nanotubes Functionalization. *Curr. Org. Chem.* **2011**, *15*, 1151–1159. [[CrossRef](#)]
184. Fan, X.; Jiao, G.; Zhao, W.; Jin, P.; Li, X. Magnetic Fe<sub>3</sub>O<sub>4</sub>-graphene composites as targeted drug nanocarriers for pH-activated release. *Nanoscale* **2013**, *5*, 1143–1152. [[CrossRef](#)]
185. Gonzalez-Rodriguez, R.; Campbell, E.; Naumov, A. Multifunctional graphene oxide/iron oxide nanoparticles for magnetic targeted drug delivery dual magnetic resonance/fluorescence imaging and cancer sensing. *PLoS ONE* **2019**, *14*, e0217072. [[CrossRef](#)]
186. Namvari, M.; Namazi, H. Clicking graphene oxide and Fe<sub>3</sub>O<sub>4</sub> nanoparticles together: An efficient adsorbent to remove dyes from aqueous solutions. *Int. J. Environ. Sci. Technol.* **2014**, *11*, 1527–1536. [[CrossRef](#)]

187. Arukali Sammaiah, A.; Huang, W.; Wang, X. Synthesis of magnetic Fe<sub>3</sub>O<sub>4</sub>/graphene oxide nanocomposites and their tribological properties under magnetic field. *Mater. Res. Express* **2018**, *5*, 105006–105015. [[CrossRef](#)]
188. Sadeghfar, F.; Ghaedi, M.; Asfaram, A.; Jannesar, R.; Javadian, H.; Pezeshkpour, V. Polyvinyl alcohol/Fe<sub>3</sub>O<sub>4</sub>@carbon nanotubes nanocomposite: Electrochemical-assisted synthesis, physicochemical characterization, optical properties, cytotoxicity effects and ultrasound-assisted treatment of aqueous based organic compound. *J. Ind. Eng. Chem.* **2018**, *65*, 349–362. [[CrossRef](#)]
189. Xu, Z.; Fan, X.; Ma, Q.; Tang, B.; Lu, Z.; Zhang, J.; Mo, G.; Ye, J.; Ye, J. A sensitive electrochemical sensor for simultaneous voltammetric sensing of cadmium and lead based on Fe<sub>3</sub>O<sub>4</sub>/multiwalled carbon nanotube/laser scribed graphene composites functionalized with chitosan modified electrode. *Mater. Chem. Phys.* **2019**, *238*, 121876–121877. [[CrossRef](#)]
190. Zhang, M.; Wang, W.; Cui, Y.; Chu, X.; Sun, B.; Zhou, N.; Shen, J. Magnetofluorescent Fe<sub>3</sub>O<sub>4</sub>/carbon quantum dots coated single-walled carbon nanotubes as dual-modal targeted imaging and chemo/photodynamic/photothermal triple-modal therapeutic agents. *Chem. Eng. J.* **2018**, *338*, 526–538. [[CrossRef](#)]
191. Zhang, W.; Li, X.; Zhou, R.; Wu, H.; Shi, H.; Yu, S.; Liu, Y. Multifunctional glucose biosensors from Fe<sub>3</sub>O<sub>4</sub> nanoparticles modified chitosan/graphene nanocomposites. *Sci. Rep.* **2015**, *5*, 11129–11138. [[CrossRef](#)]
192. Patsula, V.; Horák, D.; Kučka, J.; Mackova, H.; Lobaz, V.; Francova, P.; Herynek, V.; Heizer, T.; Paral, P.; Sefc, L. Synthesis and modification of uniform PEG-neridronate-modified magnetic nanoparticles determines prolonged blood circulation and biodistribution in a mouse preclinical model. *Sci. Rep.* **2019**, *9*, 10765–10777. [[CrossRef](#)]
193. Yuan, G.; Yuan, Y.; Xu, K.; Luo, Q. Biocompatible PEGylated Fe<sub>3</sub>O<sub>4</sub> nanoparticles as photothermal agents for near-infrared light modulated cancer therapy. *Int. J. Mol. Sci.* **2014**, *15*, 18776–18788. [[CrossRef](#)]
194. Blanco, E.; Shen, H.; Ferrari, M. Principles of nanoparticle design for overcoming biological barriers to drug delivery. *Nat. Biotechnol.* **2015**, *33*, 941–951. [[CrossRef](#)]
195. Zhou, Y.; Peng, Z.; Seven, E.S.; Leblanc, R.M. Crossing the blood-brain barrier with nanoparticles. *J. Control. Release* **2018**, *270*, 290–303. [[CrossRef](#)]
196. Suk, J.S.; Xu, Q.; Kim, N.; Hanes, J.; Ensign, L.M. PEGylation as a strategy for improving nanoparticle-based drug and gene delivery. *Adv. Drug Deliv. Rev.* **2016**, *99 Pt A*, 28–51. [[CrossRef](#)]
197. Mostaghassi, E.; Zarepour, A.; Zarrabi, A. Folic acid armed Fe<sub>3</sub>O<sub>4</sub>-HPG nanoparticles as a safe nano vehicle for biomedical theranostics. *J. Taiwan Inst. Chem. Eng.* **2018**, *82*, 33–41. [[CrossRef](#)]
198. Avedian, N.; Zaaeri, F.; Daryasari, M.P.; Javar, H.A.; Khoobi, M. pH-sensitive biocompatible mesoporous magnetic nanoparticles labeled with folic acid as an efficient carrier for controlled anticancer drug delivery. *J. Drug Deliv. Sci. Technol.* **2018**, *44*, 323–332. [[CrossRef](#)]
199. Hashemi-Moghaddam, H.; Zavareh, S.; Gazi, E.M.; Jamili, M. Assessment of novel core-shell Fe<sub>3</sub>O<sub>4</sub>@poly l-DOPA nanoparticles for targeted Taxol<sup>®</sup> delivery to breast tumor in a mouse model. *Mater. Sci. Eng. C* **2018**, *93*, 1036–1043. [[CrossRef](#)] [[PubMed](#)]
200. Wu, C.Y.; Chen, Y.C. Riboflavin immobilized Fe<sub>3</sub>O<sub>4</sub> magnetic nanoparticles carried with n-butylidene-phthalide as targeting-based anticancer agents, Artificial Cells. *Nanomed. Biotechnol.* **2019**, *47*, 210–220. [[CrossRef](#)]
201. Arriortua, O.K.; Insausti, M.; Lezama, L.; de Muro, I.G.; Garaio, E.; de la Fuente, J.M.; Fratila, R.M.; Morales, M.P.; Costa, R.; Eceiza, M.; et al. RGD-Functionalized Fe<sub>3</sub>O<sub>4</sub> nanoparticles for magnetic hyperthermia. *Colloids Surf. B Biointerfaces* **2018**, *165*, 315–324. [[CrossRef](#)] [[PubMed](#)]
202. Lu, X.; Jiang, R.; Fan, Q.; Zhang, L.; Zhang, H.; Yang, M.; Ma, Y.; Wang, L.; Huang, W. Fluorescent-magnetic poly(poly(ethyleneglycol)monomethacrylate)-grafted Fe<sub>3</sub>O<sub>4</sub> nanoparticles from post-atom-transfer-radical-polymerization modification: Synthesis, characterization, cellular uptake and imaging. *J. Mater. Chem.* **2012**, *22*, 6965–6973. [[CrossRef](#)]
203. Stephen, Z.R.; Kievit, F.M.; Zhang, M. Magnetite Nanoparticles for Medical MR Imaging. *Mater. Today* **2011**, *14*, 330–338. [[CrossRef](#)]
204. Wang, Z.; Lam, A.; Acosta, E. Suspensions of Iron Oxide Nanoparticles Stabilized by Anionic Surfactants. *J. Surfactants Deterg.* **2013**, *16*, 397–407. [[CrossRef](#)]
205. Choi, Y.W.; Lee, H.; Song, Y.; Sohn, D. Colloidal stability of iron oxide nanoparticles with multivalent polymer surfactants. *J. Colloid Interface Sci.* **2015**, *443*, 8–12. [[CrossRef](#)]



206. Zhang, Y.; Newton, B.; Lewis, E.; Fu, P.P.; Kafoury, R.; Ray, P.C.; Yu, H. Cytotoxicity of organic surface coating agents used for nanoparticles synthesis and stability. *Toxicol. Vitro*. **2015**, *29*, 762–768. [[CrossRef](#)] [[PubMed](#)]
207. Soares, P.I.P.; Lochte, F.; Echeverria, C.; Pereira, L.C.J.; Coutinho, J.T.; Ferreira, I.M.M.; Novo, C.M.M.; Borges, J.P.M.R. Thermal and magnetic properties of iron oxide colloids: Influence of surfactants. *Nanotechnology* **2015**, *26*, 425704–425715. [[CrossRef](#)] [[PubMed](#)]
208. Gonzales, M.; Mitsumori, L.M.; Kushleika, J.V.; Rosenfeld, M.E.; Krishnan, K.M. Cytotoxicity of iron oxide nanoparticles made from the thermal decomposition of organometallics and aqueous phase transfer with Pluronic F127. *Contrast Media Mol. Imaging* **2010**, *5*, 286–293. [[CrossRef](#)] [[PubMed](#)]
209. Chen, M.; Shen, H.; Li, X.; Ruan, J.; Yan, W.Q. Magnetic fluids' stability improved by oleic acid bilayer-coated structure via one-pot synthesis. *Chem. Pap.* **2016**, *70*, 1642–1648. [[CrossRef](#)]
210. Coricovac, D.E.; Moacă, E.A.; Pinzaru, I.; Citu, C.; Soica, C.; Mihail, C.V.; Pacurariu, C.; Tutelyan, V.A.; Tsatsakis, A.; Dehelean, C.A. Biocompatible Colloidal Suspensions Based on Magnetic Iron Oxide Nanoparticles: Synthesis, Characterization and Toxicological Profile. *Front. Pharmacol.* **2017**, *8*, 154–172. [[CrossRef](#)] [[PubMed](#)]
211. Mulder, W.J.M.; Strijkers, G.J.; van Tilborg, G.A.F.; Cormode, D.P.; Fayad, Z.A.; Nicolay, K. Nanoparticulate assemblies of amphiphiles and diagnostically active materials for multimodality imaging. *Acc. Chem. Res.* **2009**, *42*, 904–914. [[CrossRef](#)]
212. Yang, J.; Pinar, A. Understanding the role of grafted polystyrene chain conformation in assembly of magnetic nanoparticles. *Phys. Rev. E* **2014**, *90*, 042601.
213. Nagesha, D.K.; Plouffe, B.D.; Phan, M.; Lewis, L.H.; Sridhar, S.; Murthy, S.K. Functionalization-induced improvement in magnetic properties of Fe<sub>3</sub>O<sub>4</sub> nanoparticles for biomedical applications. *J. Appl. Phys.* **2009**, *105*, 07B317. [[CrossRef](#)]
214. Zhang, G.; Qie, F.; Hou, J.; Luo, S.; Luo, L.; Sun, X.; Tan, T. One-pot solvothermal method to prepare functionalized Fe<sub>3</sub>O<sub>4</sub> nanoparticles for bioseparation. *J. Mater. Res.* **2012**, *27*, 1006–1013. [[CrossRef](#)]
215. Ooi, F.; DuChene, J.S.; Qiu, J.; Graham, J.O.; Engelhard, M.H.; Cao, G.; Gai, Z.; Wei, W.D. A Facile Solvothermal Synthesis of Octahedral Fe<sub>3</sub>O<sub>4</sub> Nanoparticles. *Small* **2015**, *11*, 2649–2653. [[CrossRef](#)]
216. Kekalo, K.; Koo, K.; Zeitchick, E.; Baker, I. Microemulsion Synthesis of Iron Core/Iron Oxide Shell Magnetic Nanoparticles and Their Physicochemical Properties. *Mater. Res. Soc. Symp. Proc.* **2012**, *1416*, 1–11. [[CrossRef](#)] [[PubMed](#)]
217. Baharuddin, A.A.; Ang, B.C.; Hussein, N.A.A.; Andriyana, A.; Wong, Y.H. Mechanisms of highly stabilized ex-situ oleic acid-modified iron oxide nanoparticles functionalized with 4-pentynoic acid. *Mater. Chem. Phys.* **2018**, *203*, 212–222. [[CrossRef](#)]
218. Justin, C.; Samrot, A.V.; Sruthi, D.P.; Sahithya, C.S.; Bhavya, K.S.; Saipriya, C. Preparation, characterization and utilization of core-shell super paramagnetic iron oxide nanoparticles for curcumin delivery. *PLoS ONE* **2018**, *13*, e0200440. [[CrossRef](#)] [[PubMed](#)]
219. Mahdavi, M.; Ahmad, M.B.; Haron, M.J.; Namvar, F.; Nadi, B.; Rahman, M.Z.A.; Amin, J. Synthesis, Surface Modification and Characterisation of Biocompatible Magnetic Iron Oxide Nanoparticles for Biomedical Applications. *Molecules* **2013**, *18*, 7533–7548. [[CrossRef](#)] [[PubMed](#)]
220. Luchini, A.; Vitiello, G. Understanding the Nano-bio Interfaces: Lipid-Coatings for Inorganic Nanoparticles as Promising Strategy for Biomedical Applications. *Front. Chem.* **2019**, *7*, 343–359. [[CrossRef](#)]
221. Moghimi, S.M.; Szebeni, J. Stealth liposomes and long circulating nanoparticles: Critical issues in pharmacokinetics, opsonization and protein-binding properties. *Prog. Lipid Res.* **2003**, *42*, 463–478. [[CrossRef](#)]
222. Gogoi, M.; Jaiswal, M.K.; Dev Sarma, H.; Bahadur, D.; Banerjee, R. Biocompatibility and therapeutic evaluation of magnetic liposomes designed for self-controlled cancer hyperthermia and chemotherapy. *Integr. Biol.* **2017**, *9*, 555–565. [[CrossRef](#)]
223. Ramishetti, S.; Huang, L. Intelligent design of multifunctional lipid-coated nanoparticle platforms for cancer therapy. *Ther. Deliv.* **2012**, *3*, 1429–1445. [[CrossRef](#)]
224. Wijaya, A.; Hamad-Schifferli, K. High-Density Encapsulation of Fe<sub>3</sub>O<sub>4</sub> Nanoparticles in Lipid Vesicles. *Langmuir* **2007**, *23*, 9546–9550. [[CrossRef](#)]
225. Liang, J.; Zhang, X.; Miao, Y.; Li, J.; Gan, Y. Lipid-coated iron oxide nanoparticles for dual-modal imaging of hepatocellular carcinoma. *Int. J. Nanomed.* **2017**, *12*, 2033–2044. [[CrossRef](#)]



226. Radoń, A.; Drygała, A.; Hawełek, L.; Łukowiec, D. Structure and optical properties of Fe<sub>3</sub>O<sub>4</sub> nanoparticles synthesized by co-precipitation method with different organic modifiers. *Mater. Charact.* **2017**, *131*, 148–156. [[CrossRef](#)]
227. Anbarasu, M.; Anandan, M.; Chinnasamy, E.; Gopinath, V.; Balamurugan, K. Synthesis and characterization of polyethylene glycol (PEG) coated Fe<sub>3</sub>O<sub>4</sub> nanoparticles by chemical co-precipitation method for biomedical applications. *Spectrochim. Acta Mol. Biomol. Spectrosc.* **2015**, *135*, 536–539. [[CrossRef](#)] [[PubMed](#)]
228. Yang, J.; Zou, P.; Yang, L.; Cao, J.; Sun, Y.; Han, D.; Yang, S.; Wang, Z.; Chen, G.; Wang, B.; et al. A comprehensive study on the synthesis and paramagnetic properties of PEG-coated Fe<sub>3</sub>O<sub>4</sub> nanoparticles. *Appl. Surf. Sci.* **2014**, *303*, 425–432. [[CrossRef](#)]
229. Gao, G.; Qiu, P.; Qian, Q.; Zhou, N.; Wang, K.; Song, H.; Fu, H.; Cui, D. PEG-200-assisted hydrothermal method for the controlled-synthesis of highly dispersed hollow Fe<sub>3</sub>O<sub>4</sub> nanoparticles. *J. Alloys Compd.* **2013**, *574*, 340–344. [[CrossRef](#)]
230. Wang, R.; Degirmenci, V.; Xin, H.; Li, Y.; Wang, L.; Chen, J.; Hu, X.; Zhang, D. PEI-Coated Fe<sub>3</sub>O<sub>4</sub> Nanoparticles Enable Efficient Delivery of Therapeutic siRNA Targeting REST into Glioblastoma Cells. *Int. J. Mol. Sci.* **2018**, *19*, 2230. [[CrossRef](#)]
231. Ping, T.; Wang, Q.; Zhou, Y.; Nie, J. Reducing oxygen inhibition by Fe<sub>3</sub>O<sub>4</sub>@PEI nanoparticles co-initiator. *J. Photochem. Photobiol. Chem.* **2019**, *373*, 171–175. [[CrossRef](#)]
232. Sun, X.; Zheng, C.; Zhang, F.; Yang, Y.; Wu, G.; Yu, A.; Guan, N. Size-controlled synthesis of magnetite (Fe<sub>3</sub>O<sub>4</sub>) nanoparticles coated with Glucose and Gluconic Acid from a Single Fe(III) Precursor by a Sucrose Bifunctional Hydrothermal Method. *J. Phys. Chem. C* **2009**, *113*, 16002–16008. [[CrossRef](#)]
233. Sari, A.Y.; Eko, A.S.; Candra, K.; Hasibuan, D.P.; Ginting, M.; Sebayang, P.; Simamora, P. Synthesis, Properties and Application of Glucose Coated Fe<sub>3</sub>O<sub>4</sub> Nanoparticles Prepared by Co-precipitation Method. *IOP Conf. Ser. Mater. Sci. Eng.* **2017**, *214*, 012021. [[CrossRef](#)]
234. Barbaro, D.; Di Bari, L.; Gandin, V.; Evangelisti, C.; Vitulli, G.; Schiavi, E.; Marzano, C.; Ferretti, A.M.; Salvadori, P. Glucose-coated superparamagnetic iron oxide nanoparticles prepared by metal vapour synthesis are electively internalized in a pancreatic adenocarcinoma cell line expressing GLUT1 transporter. *PLoS ONE* **2015**, *10*, e0123159. [[CrossRef](#)]
235. Predescu, A.M.; Matei, E.; Berbecaru, A.C.; Pantilimon, C.; Dragan, C.; Vidu, R.; Predescu, C.; Kuncser, V. Synthesis and characterization of dextran-coated iron oxide nanoparticles. *R. Soc. Open Sci.* **2018**, *5*, 171525–171536. [[CrossRef](#)]
236. Zhang, Q.; Liu, Q.; Du, M.; Vermorken, A.; Cui, Y.; Zhang, L.; Guo, L.; Ma, L.; Chen, M. Cetuximab and Doxorubicin loaded dextran-coated Fe<sub>3</sub>O<sub>4</sub> magnetic nanoparticles as novel targeted nanocarriers for non-small cell lung cancer. *J. Magn. Magn. Mater.* **2019**, *481*, 122–128. [[CrossRef](#)]
237. Shen, M.; Yu, Y.; Fan, G.; Jin, Y.M.; Tang, W.; Jia, W. The synthesis and characterization of monodispersed chitosan-coated Fe<sub>3</sub>O<sub>4</sub> nanoparticles via a facile one-step solvothermal process for adsorption of bovine serum albumin. *Nanoscale Res. Lett.* **2014**, *9*, 296–304. [[CrossRef](#)] [[PubMed](#)]
238. Veisi, H.; Sajjadifar, S.; Biabri, P.M.; Hemmati, S. Oxo-vanadium complex immobilized on chitosan coated-magnetic nanoparticles (Fe<sub>3</sub>O<sub>4</sub>): A heterogeneous and recyclable nanocatalyst for the chemoselective oxidation of sulfides to sulfoxides with H<sub>2</sub>O<sub>2</sub>. *Polyhedron* **2018**, *153*, 240–247. [[CrossRef](#)]
239. Lotfi, S.; Bahari, A.; Mahjoub, S. In vitro biological evaluations of Fe<sub>3</sub>O<sub>4</sub> compared with core-shell structures of chitosan-coated Fe<sub>3</sub>O<sub>4</sub> and polyacrylic acid-coated Fe<sub>3</sub>O<sub>4</sub> nanoparticles. *Res. Chem. Intermed.* **2019**, *45*, 3497–3512. [[CrossRef](#)]
240. Illés, E.; Szekeres, M.; Tóth, I.Y.; Farkas, K.; Foeldes, I.; Szabo, A.; Ivan, B.; Tombacz, E. PEGylation of Superparamagnetic Iron Oxide Nanoparticles with Self-Organizing Polyacrylate-PEG Brushes for Contrast Enhancement in MRI Diagnosis. *Nanomaterials* **2018**, *8*, 776. [[CrossRef](#)]
241. Illés, E.; Szekeres, M.; Tóth, I.Y.; Szabó, Á.; Iván, B.; Turcu, R.; Vékás, L.; Zupkó, I.; Jaics, G.; Tombacz, E. Multifunctional PEG-carboxylate copolymer coated superparamagnetic iron oxide nanoparticles for biomedical application. *J. Magn. Magn. Mater.* **2018**, *451*, 710–720. [[CrossRef](#)]
242. Iglesias, G.R.; Reyes-Ortega, F.; Checa Fernandez, B.L.; Delgado, Á.V. Hyperthermia-Triggered Gemcitabine Release from Polymer-Coated Magnetite Nanoparticles. *Polymers* **2018**, *10*, 269. [[CrossRef](#)]
243. Dutta, B.; Shetake, N.G.; Gawali, S.L.; Barick, B.K.; Barick, K.C.; Babu, P.D.; Pandey, B.N.; Priyadarsini, K.I.; Hassan, P.A. PEG mediated shape-selective synthesis of cubic Fe<sub>3</sub>O<sub>4</sub> nanoparticles for cancer therapeutics. *J. Alloys Compd.* **2018**, *737*, 347–355. [[CrossRef](#)]

244. You, L.; Liu, X.; Fang, Z.; Xu, Q.; Zhang, Q. Synthesis of multifunctional Fe<sub>3</sub>O<sub>4</sub>@PLGA-PEG nano-niosomes as a targeting carrier for treatment of cervical cancer. *Mater. Sci. Eng.* **2019**, *94*, 291–302. [[CrossRef](#)]
245. Sun, X.; Shen, J.; Yu, D.; Ouyang, X. Preparation of pH-sensitive Fe<sub>3</sub>O<sub>4</sub>@C/carboxymethyl cellulose/chitosan composite beads for diclofenac sodium delivery. *Int. J. Biol. Macromol.* **2019**, *127*, 594–605. [[CrossRef](#)]
246. Sakaguchi, M.; Makino, M.; Ohura, T.; Yamamoto, K.; Enomoto, Y.; Takase, H. Surface modification of Fe<sub>3</sub>O<sub>4</sub> nanoparticles with dextran via a coupling reaction between naked Fe<sub>3</sub>O<sub>4</sub> mechano-cation and naked dextran mechano-anion: A new mechanism of covalent bond formation. *Adv. Powder Technol.* **2019**, *30*, 795–806. [[CrossRef](#)]
247. Wang, F.; Li, X.; Li, W.; Bai, H.; Gao, Y.; Ma, J.; Liu, W.; Xi, G. Dextran coated Fe<sub>3</sub>O<sub>4</sub> nanoparticles as a near-infrared laser-driven photothermal agent for efficient ablation of cancer cells in vitro and in vivo. *Mater. Sci. Eng.* **2018**, *90*, 46–56. [[CrossRef](#)] [[PubMed](#)]
248. Banobre-Lopez, M.; Pineiro-Redondo, Y.; Sandri, M.; Tampieri, A.; De Santis, R.; Dediu, V.A.; Rivas, J. Hyperthermia Induced in Magnetic Scaffolds for Bone Tissue Engineering. *IEEE Trans. Magn.* **2014**, *50*, 1–7. [[CrossRef](#)]
249. Lai, W.Y.; Feng, S.W.; Chan, Y.H.; Chang, W.J.; Wang, H.T.; Huang, H.M. In Vivo Investigation into Effectiveness of Fe<sub>3</sub>O<sub>4</sub>/PLLA Nanofibers for Bone Tissue Engineering Applications. *Polymers* **2018**, *10*, 804. [[CrossRef](#)]
250. Maier-Hauff, K.; Rothe, R.; Scholz, R.; Gneveckow, U.; Wust, P.; Thiesen, B.; Feussner, A.; von Deimling, A.; Waldoefner, N.; Felix, R.; et al. Intracranial thermotherapy using magnetic nanoparticles combined with external beam radiotherapy: Results of a feasibility study on patients with glioblastoma multiforme. *J. Neurooncol.* **2007**, *81*, 53–60. [[CrossRef](#)]
251. Maier-Hauff, K.; Ulrich, F.; Nestler, D.; Niehoff, H.; Wust, P.; Thiesen, B.; Orawa, H.; Budach, V.; Jordan, A. Efficacy and safety of intratumoral thermotherapy using magnetic iron-oxide nanoparticles combined with external beam radiotherapy on patients with recurrent glioblastoma multiforme. *J. Neurooncol.* **2011**, *103*, 317–324. [[CrossRef](#)]
252. Grauer, O.; Jaber, M.; Hess, K.; Weckesser, M.; Schwindt, W.; Maring, S.; Woelfer, J.; Stummer, W. Combined intracavitary thermotherapy with iron oxide nanoparticles and radiotherapy as local treatment modality in recurrent glioblastoma patients. *J. Neurooncol.* **2019**, *141*, 83–84. [[CrossRef](#)]
253. Chatterjee, D.K.; Diagaradjane, P.; Krishnan, S. Nanoparticle-mediated hyperthermia in cancer therapy. *Ther. Deliv.* **2011**, *2*, 1001–1014. [[CrossRef](#)]
254. Goya, G.F.; Lima, E., Jr.; Arelaro, A.D.; Torres, T.E.; Rechenberg, H.R.; Rossi, L.; Marquina, C.; Ibarra, M.R. Magnetic Hyperthermia with Fe<sub>3</sub>O<sub>4</sub> nanoparticles: The Influence of Particle Size on Energy Absorption. *IEEE Trans. Magn.* **2008**, *44*, 4444–4447. [[CrossRef](#)]
255. Kaur, P.; Aliru, M.L.; Chadha, A.S.; Asea, A.; Krishnan, S. Hyperthermia using nanoparticles—Promises and pitfalls. *Int. J. Hyperth.* **2016**, *32*, 76–88. [[CrossRef](#)]
256. Temelie, M.; Popescu, R.C.; Cocioaba, D.; Vasile, B.S.; Savu, D. Biocompatibility study of magnetite nanoparticles synthesized using a green method. *Rom. J. Phys.* **2018**, *63*, 703–716.
257. Rasouli, E.; Basirun, W.J.; Rezayi, M.; Shameli, K.; Nourmohammadi, E.; Khandanlou, R.; Izadiyan, Z.; Sarkarizi, H.K. Ultrasmall superparamagnetic Fe<sub>3</sub>O<sub>4</sub> nanoparticles: Honey-based green and facile synthesis and in vitro viability assay. *Int. J. Nanomed.* **2018**, *2018*, 6903–6911. [[CrossRef](#)] [[PubMed](#)]
258. Sathishkumar, G.; Logeshwaran, V.; Sarathbabu, S.; Jha, P.K.; Jeyaraj, M.; Rajkuberan, C.; Senthilkumar, N.; Sivaramakrishnan, S. Green synthesis of magnetic Fe<sub>3</sub>O<sub>4</sub> nanoparticles using Couroupitaguianensis Aubl. fruit extract for their antibacterial and cytotoxicity activities. *Artif. Cells Nanomed. Biotechnol.* **2018**, *46*, 589–598. [[CrossRef](#)] [[PubMed](#)]
259. Chifiriuc, C.; Grumezescu, V.; Grumezescu, A.M.; Saviuc, C.; Lazăr, V.; Andronescu, E. Hybrid magnetite nanoparticles/Rosmarinus officinalis essential oil nanobiosystem with antibiofilm activity. *Nanoscale Res. Lett.* **2012**, *7*, 209–216. [[CrossRef](#)]
260. Rădulescu, M.; Andronescu, E.; Holban, A.M.; Vasile, B.S.; Iordache, F.; Mogoantă, L.; Mogoșanu, G.D.; Grumezescu, A.M.; Georgescu, M.; Chifiriuc, M.C. Antimicrobial Nanostructured Bioactive Coating Based on Fe<sub>3</sub>O<sub>4</sub> and Patchouli Oil for Wound Dressing. *Metals* **2016**, *6*, 103. [[CrossRef](#)]
261. Sadeghzadeh, H.; Pilehvar-Soltanahmadi, Y.; Akbarzadeh, A.; Dariushnejad, H.; Sanjarian, F.; Zarghami, N. The Effects of Nanoencapsulated Curcumin-Fe<sub>3</sub>O<sub>4</sub> on Proliferation and hTERT Gene Expression in Lung Cancer Cells. *Anti-Cancer Agents Med. Chem.* **2017**, *17*, 1363–1373. [[CrossRef](#)]

262. Ruíz-Baltazar, A.J.; Reyes-López, S.Y.; Mondragón-Sánchez, M.L.; Robles-Cortés, A.I.; Pérez, R. Eco-friendly synthesis of Fe<sub>3</sub>O<sub>4</sub> nanoparticles: Evaluation of their catalytic activity in methylene blue degradation by kinetic adsorption models. *Res. Phys.* **2019**, *12*, 989–995. [[CrossRef](#)]
263. Yew, Y.P.; Shameli, K.; Miyake, M.; Kuwano, N.; Khairudin, N.B.B.A.; Mohamad, S.E.B.; Lee, K.X. Green Synthesis of Magnetite (Fe<sub>3</sub>O<sub>4</sub>) Nanoparticles Using Seaweed (*Kappaphycus alvarezii*) Extract. *Nanoscale Res. Lett.* **2016**, *11*, 276–283. [[CrossRef](#)]
264. Hosseini, A.; Ghorbani, A. Cancer therapy with phytochemicals: Evidence from clinical studies. *Avicenna J. Phytomed.* **2015**, *5*, 84–97.
265. Shivani Thoidingjam, S.; Tiku, A.B. Therapeutic efficacy of Phyllanthus emblica-coated iron oxide nanoparticles in A549 lung cancer cell line. *Nanomedicine* **2019**, *14*, 2355–2371. [[CrossRef](#)]
266. Ramirez-Nuñez, A.L.; Jimenez-Garcia, L.F.; Goya, G.F.; Sanz, B.; Santoyo-Salazar, J. In vitro magnetic hyperthermia using polyphenol-coated Fe<sub>3</sub>O<sub>4</sub>@γ-Fe<sub>2</sub>O<sub>3</sub> nanoparticles from Cinnamomum verum and Vanilla planifolia: The concert of green synthesis and therapeutic possibilities. *Nanotechnology* **2018**, *29*, 074001. [[CrossRef](#)] [[PubMed](#)]
267. Lewinska, A.; Adamczyk-Grochala, J.; Bloniarz, D.; Olszowka, J.; Kulpa-Greszta, M.; Litwinienko, G.; Tomaszewska, A.; Wnuk, M.; Pazik, R. AMPK-mediated senolytic and senostatic activity of quercetin surface functionalized Fe<sub>3</sub>O<sub>4</sub> nanoparticles during oxidant-induced senescence in human fibroblasts. *Redox Biol.* **2020**, *28*, 101337. [[CrossRef](#)] [[PubMed](#)]
268. Ebrahimipour, S.; Esmaeili, A.; Beheshti, S. Effect of quercetin-conjugated superparamagnetic iron oxide nanoparticles on diabetes-induced learning and memory impairment in rats. *Int. J. Nanomed.* **2018**, *2018*, 6311–6324. [[CrossRef](#)] [[PubMed](#)]
269. Dorniani, D.; Hussein, M.Z.; Kura, A.U.; Fakurazi, S.; Shaari, A.H.; Ahmad, Z. Preparation of Fe<sub>3</sub>O<sub>4</sub> magnetic nanoparticles coated with gallic acid for drug delivery. *Int. J. Nanomed.* **2012**, *7*, 5745–5756. [[CrossRef](#)] [[PubMed](#)]
270. Li, L.; Gao, F.; Jiang, W.; Wu, X.; Cai, Y.; Tang, J.; Gao, X.; Gao, F. Folic acid-conjugated superparamagnetic iron oxide nanoparticles for tumor-targeting MR imaging. *Drug Deliv.* **2016**, *23*, 1726–1733. [[CrossRef](#)] [[PubMed](#)]
271. Choi, K.H.; Nam, K.C.; Cho, G.; Jung, J.S.; Park, B.J. Enhanced Photodynamic Anticancer Activities of Multifunctional Magnetic Nanoparticles (Fe<sub>3</sub>O<sub>4</sub>) Conjugated with Chlorin e6 and Folic Acid in Prostate and Breast Cancer Cells. *Nanomaterials* **2018**, *8*, 722. [[CrossRef](#)]
272. Popescu, R.C.; Andronescu, E.; Vasile, B.S.; Trusca, R.; Boldeiu, A.; Mogoanta, L.; Mogosanu, G.D.; Temelie, M.; Radu, M.; Grumezescu, A.M.; et al. Fabrication and Cytotoxicity of Gemcitabine-Functionalized Magnetite Nanoparticles. *Molecules* **2017**, *22*, 1080. [[CrossRef](#)]
273. Zhang, Q.; Liu, J.; Yuan, K.; Zhang, Z.; Zhang, X.; Fang, X. A multi-controlled drug delivery system based on magnetic mesoporous Fe<sub>3</sub>O<sub>4</sub> nanoparticles and a phase change material for cancer thermo-chemotherapy. *Nanotechnology* **2017**, *28*, 405101–405131. [[CrossRef](#)]
274. Xia, K.; Lyu, Y.; Yuan, W.; Wang, G.; Stratton, H.; Zhang, S.; Wu, J. Nanocarriers of Fe<sub>3</sub>O<sub>4</sub> as a Novel Method for Delivery of the Antineoplastic Agent Doxorubicin into HeLa Cells in vitro. *Front. Oncol.* **2019**, *9*, 250–257. [[CrossRef](#)]
275. Hu, X.; Wang, Y.; Zhang, L.; Xu, M.; Zhang, J.; Dong, W. Dual-pH/Magnetic-Field-Controlled Drug Delivery Systems Based on Fe<sub>3</sub>O<sub>4</sub>@SiO<sub>2</sub>-Incorporated Saiecan Graft Copolymer Composite Hydrogels. *ChemMedChem* **2017**, *12*, 1600–1609. [[CrossRef](#)]

